2008-01-0194

The Influence of Vehicle-to-Ground Impact Conditions on Rollover Dynamics and Severity

Nathan A. Rose
Gray Beauchamp
Stephen J. Fenton
Kineticorp, LLC

ABSTRACT

This paper explores the influence of the impact conditions on the dynamics and the severity of rollover crashes. Causal connections are sought between the impact conditions and the crash attributes to which they lead. The paper begins by extending previously presented equations that describe the dynamics of an idealized vehicle-to-ground impact. It then considers the behavior of these equations under a variety of impact conditions that occur during real-world rollovers. Specifically, the equations of this impact model are used to explore the ways in which and the extent to which rollover dynamics and severity are influenced by the following factors: (1) the vehicle's shape and its orientation at impact, (2) its weight, center-of-mass location, and roll moment of inertia, (3) its translational speed, (4) its downward velocity, and (5) its roll velocity. Throughout this discussion, data from real-world and staged rollover crashes is used to give the parameter study an empirical basis.

INTRODUCTION

PURPOSE

A rollover crash consists of a series of vehicle-to-ground impacts separated by periods of airborne motion. The specific conditions of the impacts, including the initial velocities and the vehicle's inertial, geometric and structural properties, will determine the forces to which the vehicle is subjected and the roll motion that results. This paper explores the influence of the impact conditions on the dynamics and the severity of rollover crashes. Causal connections are sought between the impact conditions and the crash attributes to which they lead. This paper is inclined towards theoretical reasoning and discussion, though there is a considerable amount of empirical data referenced in the text. While this theoretical dominance may at times frustrate the reader, the authors feel strongly that theoretical modeling can offer insight that may form the basis for an insightful interpretation of empirical data. Also, a theoretical model must ultimately drive causal reasoning. As is often stated, correlation does not establish causation. Some type of theoretical reasoning is necessary to understand the ways in which correlated variables might be causally related.

In a previous paper [25], the authors presented a planar, vehicle-to-ground impact model derived using the principle of impulse and momentum and based on the idealized vehicle-to-ground impact shown in Figure 1.

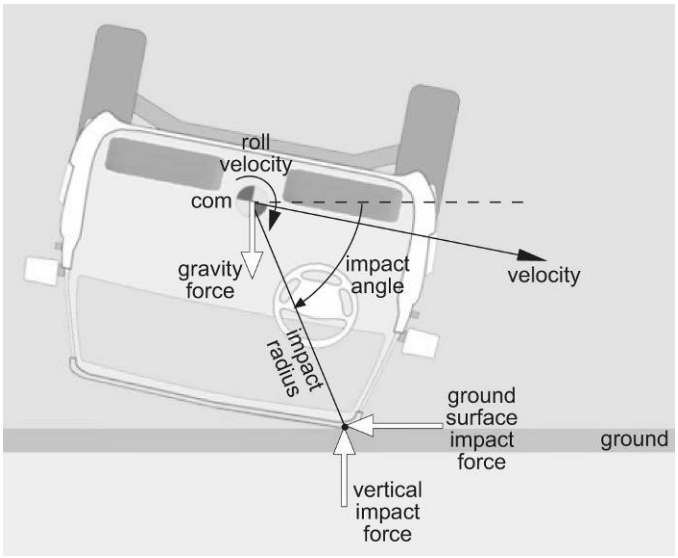

Figure 1

The vehicle in this figure is depicted in an inverted orientation with the driver's side roof impacting the ground. The vehicle has velocity both along and into the ground and a roll velocity that contributes to the speed with which the roof impacts the ground. As a result of this impact, the vehicle is subjected to an impact force that consists of both vertical and ground surface components. The geometry of this impact is defined by the impact radius, which is the distance from the vehicle center-of-mass (CoM) to the point at which the impact force is applied, and the impact angle, which is the angle

between the ground plane and the impact radius. Though depicted as a roof-to-ground impact in the image to the right, the equations of this impact model are equally applicable to other types of vehicle-to-ground impacts, such as wheel-to-ground impacts.

The discussion in this paper begins by extending the previously presented equations that describe the dynamics of this idealized impact. It then considers the behavior of these equations under a variety of impact conditions that occur during real-world rollovers. Specifically, the equations of this impact model are used to explore the ways in which and the extent to which rollover dynamics and severity are influenced by the following factors: (1) the vehicle's shape and its orientation at impact [represented by the impact angle and impact radius], (2) its weight, center-of-mass location, and roll moment of inertia [represented by the radius of gyration and the impact radius], (3) its translational speed, (4) its downward velocity, and (5) its roll velocity. Throughout our discussion, we draw on data from real-world and staged rollover crashes in order to give our theoretical parameter study an empirical basis.

CLARIFYING NOTE ON SEVERITY

Within the context of motor vehicle crashes, the term *severity* can be defined in two ways. First, severity can refer to a characteristic of a crash that predicts the probability a vehicle occupant in that crash will be injured. The change in velocity experienced by a vehicle during a front, side or rear impact often serves as this type of severity metric [18, 22]. Defined in this way, one crash can be said to be more severe than another because it carries with it a higher probability of occupant injury.

The term severity can also refer to the energy absorption demands placed on the vehicle structure during a crash. Under this definition, the severity of a crash increases as the magnitude of the energy absorption demand increases. This definition of severity should not be interpreted to imply a direct link between vehicle deformation and crash severity. Particularly within the context of rollover crashes, it is essential to observe that identical vehicles subjected to rollover crashes of similar severity can experience significantly different deformation patterns because of differences in how impact forces are distributed over the vehicle structure [13]. For example, a roof-to-ground impact that concentrates the impact force on a single roof pillar will generally result in a greater depth of roof pillar deformation than an impact of similar severity that engages multiple pillars.

This paper considers the severity of vehicle-to-ground impacts in the following terms: (1) the vertical change in velocity experienced by the vehicle's CoM during the impact, (2) the ground surface change in velocity experienced by the vehicle's CoM, (3) the vehicle's change in roll velocity, (4) the change in velocity experienced by the vehicle in the area where it contacts the ground. and (5) the energy dissipated during the impact. These severity metrics clearly relate to the forces applied to the vehicle during the impact. Though no attempt is made in this paper to correlate any of these severity metrics to occupant injury potential, there is reason to believe that they also relate to occupant injury potential during any particular vehicle-to-ground impact. For instance, Orlowski, Bundorf and Moffatt [19] observed in relationship to the Malibu test series that "in the majority of the ground impacts, the dummy essentially remained in contact with the same part of the vehicle perimeter and simply pressed harder against it as the vehicle struck the ground. Consequently, the change in velocity of that portion of the vehicle against which the dummy was touching determined the change in velocity of the dummy through that impact. It was the change in velocity rather than acceleration of the dummy which was the critical measure of the impact severity in these tests."

A number of studies that have sought causes of occupant injuries in rollovers have focused on crash attributes or outcomes – the number of quarter rolls [13], the initial vehicle translational speed [16], and the magnitude of roof deformation [11] or post-crash headroom [21] – and on how those attributes correlate to injury rates. But crash attributes and outcomes are not causes. In fact, they are effects that result from a combination of the rollover initial conditions and the particular forces to which the vehicle is subjected during the rollover. It is these initial conditions and underlying forces that cause certain crash attributes or outcomes to be present. If there is a correlation between certain injury types and a particular crash attribute, it is the underlying forces that cause this crash attribute to be present that could also relate to the actual cause of that injury type. Thus, an understanding of the initial conditions and underlying forces causing certain crash attributes may be significant to reducing injury potential in rollovers, for as Barrentine [2] has observed: "To control the response, one must control the causes." The research reported here examines those underlying forces and the rollover dynamics they produce, and thus, this research may ultimately have relevance to interpreting studies exploring the connection between crash attributes or outcomes and injury rates.

VEHICLE-TO-GROUND IMPACT MODEL

Figure 2 again depicts an idealized impact between a vehicle and the ground. In this figure, however, the descriptive labels of the previous figures have been replaced with the symbols which will be used in the impact model equations. The impact angle and impact radius are designated with the symbols ϕ and r. The velocity vector is designated with the letter v and the vehicle's roll velocity is designated ω_r. During the depicted impact, the vehicle is subjected to both upward and ground surface impact force components, $F_{vertical}$

and F_{ground}, and the gravity force, which is the vehicle's weight. In general, F_{ground} can act in either the positive (left) or negative (right) direction. On the other hand, $F_{vertical}$ will always act in the positive-z direction and the gravity force will always act in the negative-z direction.

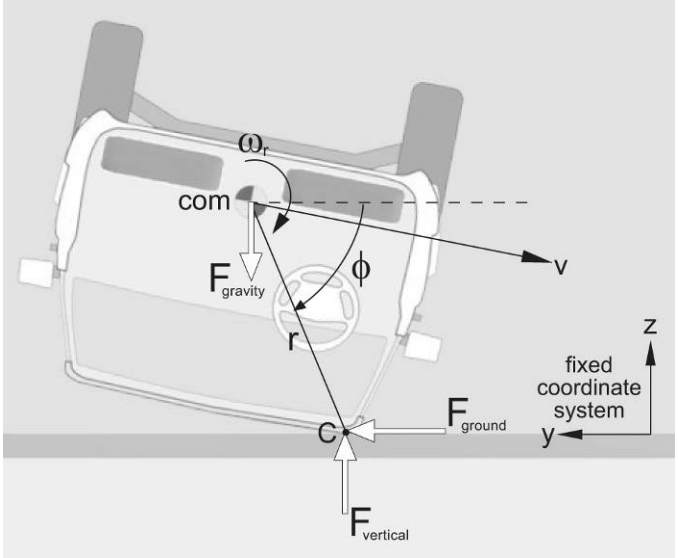

Figure 2

IMPACT MODEL ASSUMPTIONS

Before discussing equations that will yield the velocity changes and energy loss for the impact of Figure 2, first consider the assumptions that the mathematics of those equations invoke. These assumptions include the following:

1. The impact has been assumed to occur entirely in a single plane, and thus, velocity changes along the vehicle's longitudinal axis are neglected, as are changes in pitch and yaw velocity.

2. The impact model equations recognize no change in the position of the vehicle through the impact.

3. The impact force has been assumed to be concentrated at a single point.

4. It has been assumed that no moment arises at the contact point.

5. Any effects of ground plane restitution have been neglected. In other words, the ground surface impact force has been assumed to be a retarding force that depends on relative velocity at the contact point for its development. It is assumed that there is no structural restitution that could potentially cause a velocity reversal in the contact region.

The meaning of the first three of these assumptions should be relatively clear. We suspect that the meaning of the last two will be less clear, and thus, we refer the reader to the extensive discussion of these concepts in the text by Brach, titled Mechanical Impact Dynamics [3, 7]. Relaxing these last two assumptions is possible. However, in our judgment, this would make the modeling reported in this paper needlessly complex.

All five of these assumptions have the potential to be violated during any particular vehicle-to-ground impact. The degree to which any one of them is an appropriate assumption will depend on the specifics of the particular vehicle-to-ground impact under consideration and on the degree to which violating any of these assumptions will actually degrade the accuracy of the results the impact model yields. The authors have begun examining these issues in a companion paper forthcoming through SAE [26].

IMPACT MODEL EQUATIONS

Application of the principle of impulse and momentum for the idealized impact of Figure 2 results in the following equations, which yield the vehicle's upward and ground plane CoM velocity changes and the vehicle's change in roll velocity [25].[1] A full derivation of these equations is provided in Appendix A.

$$\Delta V_z = -(1+e)\cdot v_{zc,i}\cdot\left\{\frac{k_r^2}{k_r^2 + r^2\left(c^2\phi - \mu\cdot s\phi\cdot c\phi\right)}\right\} - g\cdot\Delta t_i\cdot\left\{\frac{r^2\left(c^2\phi - \mu\cdot s\phi\cdot c\phi\right)}{k_r^2 + r^2\left(c^2\phi - \mu\cdot s\phi\cdot c\phi\right)}\right\} \quad (1)$$

$$\Delta V_y = \mu\cdot\left(\Delta V_z + g\cdot\Delta t_i\right) \quad (2)$$

$$\Delta\omega_r = \left(\Delta V_z + g\cdot\Delta t_i\right)\cdot\frac{r\cdot\left(\mu\cdot s\phi - c\phi\right)}{k_r^2} \quad (3)$$

In these equations, $v_{zc,i}$ is the vertical velocity of the vehicle at Point C immediately preceding the ground contact, k_r is the vehicle's radius of gyration for the roll axis, g is the gravitational constant, Δt_i is the duration of the impact, and the letters s and c designate the sine and cosine. Note that although the collision force has been assumed to be transferred without any movement of the vehicle, accounting for the effect of the gravity impulse has required inclusion of the impact duration [10].

Examination of Equations (1) through (3) reveals that the initial downward velocity at the Point C ($v_{zc,i}$) directly influences the velocity changes that occur during the impact, with the velocity changes increasing as this velocity increases. This initial vertical velocity at Point C, which is given by the following equation, is related to the vehicle's CoM vertical velocity ($v_{z,i}$), its roll velocity ($\omega_{r,i}$) and the impact angle and radius:

[1] The authors presented these equations in Reference 25. However, in that reference, Equation (2) failed to include the gravity term.

$$v_{zc,i} = v_{z,i} - r \cdot c\phi \cdot \omega_{r,i} \quad (4)$$

Equations (1) through (3) also include the coefficient of restitution, e, and the impulse ratio, μ. The coefficient of restitution is the negative ratio of the post-impact to the pre-impact vertical velocity at Point C. The impulse ratio is the ratio of the ground plane collision impulse to the vertical direction collision impulse. In some instances, the impulse ratio can be thought of as a coulomb friction value, though its application is not limited to this interpretation [3, 4, 5, 6, 17]. In addition to the effects of friction between the ground and the vehicle body, the ground plane impulse may also include the effects of forces generated by snagging between the vehicle and the ground or furrowing of the vehicle into the ground. The "available friction" can be set at a value that reflects such snagging or furrowing when it occurs.

Within this impact model, the sign of the impulse ratio governs the direction in which the ground plane collision force acts. A positive impulse ratio produces a ground plane force that acts in the positive direction and a negative impulse ratio results in a ground plane force that acts in the negative direction. The direction of the ground plane impact force, in turn, determines whether the vehicle will experience a positive or negative ground plane velocity change and whether the ground surface impact force will tend to increase or decrease the roll velocity. For the passenger side leading roll depicted in the images of this paper, a positive F_{ground} will act to accelerate the roll and a negative F_{ground} will act to decelerate the roll. This trend will be reversed for a driver's side leading roll.

Physically, the ground plane impulse will act in a direction opposing the velocity of the vehicle in its region of contact with the ground (Figures 3a and 3b) [9]. Thus, the impulse ratio can be further specified with the following equation:

$$\mu = -\mu_0 \cdot sign\left(v_{yc,i}\right) \quad (5)$$

In this equations, μ_0 is the nominal value of the impulse ratio that defines the magnitude of the ground plane impulse relative to the vertical impulse and $v_{yc,i}$ is the ground plane velocity of the vehicle at Point C. This velocity is given by the following equation:

$$v_{yc,i} = v_{y,i} + r \cdot s\phi \cdot \omega_{r,i} \quad (6)$$

Thus, for a particular vehicle-to-ground impact, the relative magnitude of the vehicle's CoM ground plane velocity ($v_{y,i}$) and the ground plane component of its rotational perimeter velocity ($r \cdot s\phi \cdot \omega_{r,i}$) will determine the sign of $v_{yc,i}$ and, thus, the sign of μ.

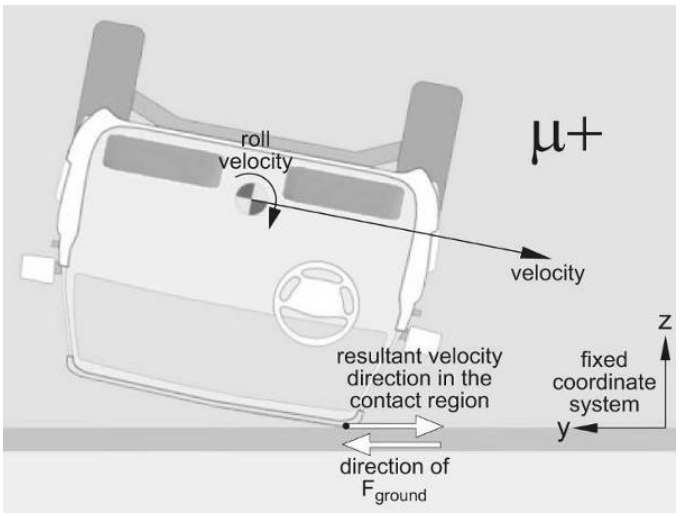

Figure 3a

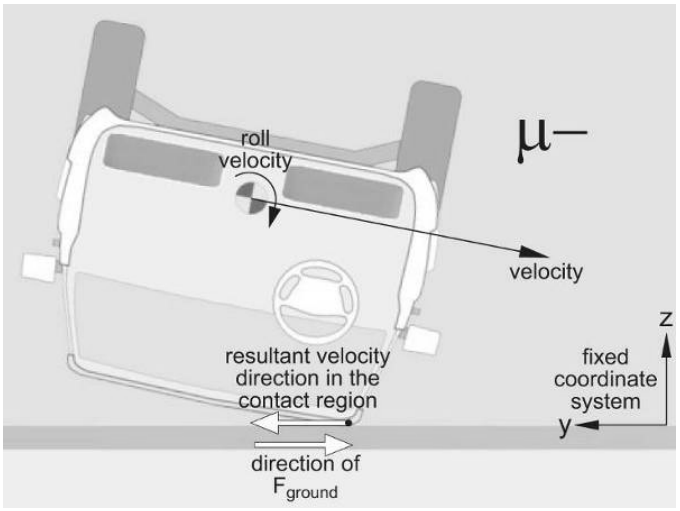

Figure 3b

At this point, it is important to state that the impact angle, ϕ, does not directly describe the vehicle's roll orientation at the time of a vehicle-to-ground impact. When the analyst places the Point C, the impact angle that results is only partly related to the roll angle. It also depends on other factors such as the amount of deformation that occurs during the impact. To see this, consider Figure 4. This figure depicts three roof-to-ground impacts that occur with identical roll angles, but with roof deformation magnitudes that vary. The roof deformation for these three impacts increases from left-to-right. For each of these impacts, the Point C has been positioned at the center of the deformation region. In this case, increasing deformation has resulted in an increasing impact angle and a decreasing impact radius.

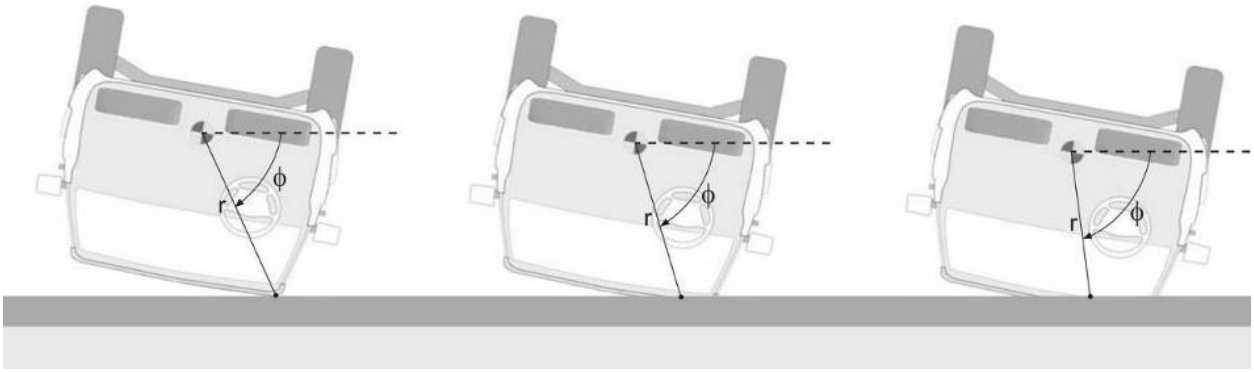

Figure 4

In addition to the CoM velocity changes given by Equations (1) and (2), the velocity changes occurring at the vehicle-to-ground impact point may have significance to assessing the severity of a vehicle-to-ground impact. Equations (7) and (8) yield the ground plane and vertical components of this velocity change that would occur at the impact point.

$$\Delta V_{y,c} = \Delta V_y + r \cdot s\phi \cdot \Delta\omega_r \quad (7)$$

$$\Delta V_{z,c} = \Delta V_z - r \cdot c\phi \cdot \Delta\omega_r \quad (8)$$

Finally, the energy loss that occurs during a vehicle-to-ground impact can be written as follows:

$$E_d = \frac{m}{2} \cdot \left(v_{zi}^2 - v_{zf}^2 + v_{yi}^2 - v_{yf}^2 + k_r^2 \omega_{r,i}^2 - k_r^2 \omega_{r,f}^2 \right) \quad (9)$$

The energy loss of Equation (9) includes the energy loss due to vehicle deformation, ground deformation, and sliding, snagging or furrowing between the vehicle structure and the ground.

IMPACT MODEL PARAMETER STUDY

THE FACTORS AND THEIR LEVELS

This section focuses on establishing appropriate levels (ranges) for each of the factors that influence the behavior of Equations (1) through (9). In setting levels for each factor, our first goal was to establish physically realistic ranges. Our second goal was to avoid artificially restricting the ranges in a way that would cause misunderstanding of the behavior of Equations (1) through (9). In this regard, we attempt to follow Larry Barrentine's [2] advice: "Set levels boldly without being careless. One needs levels as wide as reasonable to force effects to show themselves." That said, in order to keep the parameter study results to a manageable level, we do restrict the ranges of variables that have a straightforward influence within the impact model equations.

Table 1 lists the factors that influence the behavior of Equations (1) through (9) along with the method that will be used to establish a range for each factor.

Factor	Method of Establishing Range
Translational Speed	Determine from Real-World Crashes and Crash Test Data
Downward Velocity at the CoM	Determine from Real-World Crashes and Crash Test Data
Roll Velocity	Determine from Real-World Crashes and Crash Test Data
Radius of Gyration and Vehicle Geometry	Determine from NHTSA Inertial Parameter Data
Impact Radius	Maximum Radius Defined by Vehicle Geometry
Impact Angle	Defined by Geometry and Limited by Physical Constraints
Coefficient of Restitution	Assume e=0 (See discussion below.)
Impulse Ratio	Assume Available Friction Coefficient, μ=0.5
Impact Duration	Determine from Crash Tests

TABLE 1

Translational Speed and Roll Velocity

SAE Paper Number 2007-01-0726 discussed the dynamics of 12 real-world rollover crashes that were captured on video [25]. The characteristics of these crashes provide a basis on which to establish a range for several of the factors listed in the table above. For instance, consider the dynamics of Case #3 from 2007-01-0726, a high-speed, multiple-roll, crash involving a GMC Yukon Denali. Figure 5 contains frames from the video of this case showing the roll motion of the vehicle in this crash.

Figure 5

Based on analysis of this video, the authors estimated that this vehicle rolled for a distance of approximately 144 feet and that it had a translational speed at the beginning of the roll of around 48 mph (deceleration rate = 0.53). Figure 6 depicts the roll velocity curve for this crash, plotted with the progression of the 3-¾ rolls that the vehicle experienced. After completing ¼-roll, the roll velocity of the vehicle was around 200 degrees per second. By the time the vehicle completed its first roll, the roll velocity had increased to around 450 degrees per second. Roll velocities exceeding 400 degrees per second were then maintained nearly through the third roll. From that point forward, the roll velocity generally decreased until the vehicle came to rest.

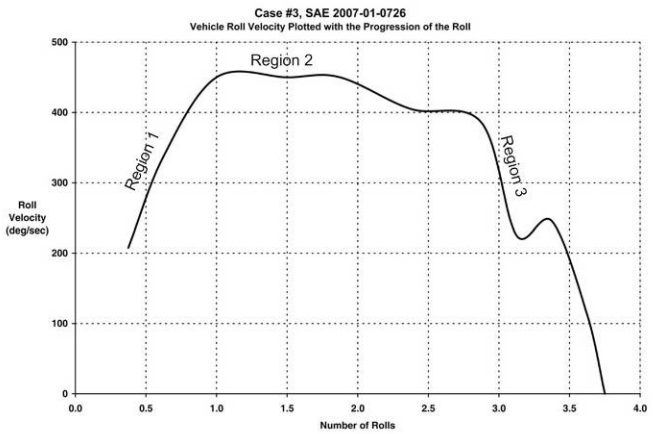

Figure 6

The roll velocity time history for this crash is similar to that for other high-speed, multiple roll crashes that the authors presented in SAE 2007-01-0726. For instance, consider the roll velocity time histories for Case Numbers 1, 6, 7 and 11, shown in Figure 7. In each of these cases, the roll velocity reached a moderate level after the vehicle completed about ¼-roll (the beginning of the roll phase), then builds up to a high roll velocity level (400 deg/sec or higher). For three out these four cases, high roll velocities are then maintained for some period of time before the roll velocity begins to diminish prior to the vehicle coming to rest.

Assuming that these vehicles' translational speeds started high and steadily diminishes throughout the rollover, these roll velocity time histories for these five high-speed rollover crashes can conceptually be split into the following three regions:

- **Region 1** – Moderate to High Roll Velocities Occurring at High Translational Speeds
- **Region 2** – High Roll Velocities Occurring at Moderate Translational Speeds
- **Region 3** – High to Low Roll Velocities Occurring at Low Translational Speeds

These regions have been identified on the roll velocity time histories of Figure 6 and 7. In our experience, vehicles involved in high-speed, multiple-roll crashes that are similar to these ones generally begin rolling with translational speeds between 30 and 65 mph and with roll velocities between 200 and 400 degrees per second. Peak roll velocities for these crashes generally fall between 400 and 700 degrees per second. In terms of the shape of the roll velocity time history for these high-speed rollover crashes, the duration of Region 2 is generally the most variable, with some crashes having no such region (Case #1, for instance).

Given these considerations, the following set of velocity conditions was chosen for the parameter study presented later:

- Translational Speed = 40 mph, Roll Velocities between 200 and 600 deg/s (Region 1)
- Translational Speed = 30 mph, Roll Velocities between 200 and 600 deg/s (Region 1 or 2)

- Translational Speed = 20 mph, Roll Velocities between 200 and 600 deg/s (Region 2 or 3)
- Translational Speed = 10 mph, Roll Velocities between 200 and 600 deg/s (Region 3)

These velocity conditions span the three translational speed/roll velocity regions identified above and, thus, they will allow for consideration of how the outcome of a vehicle-to-ground impact depends on these regions.

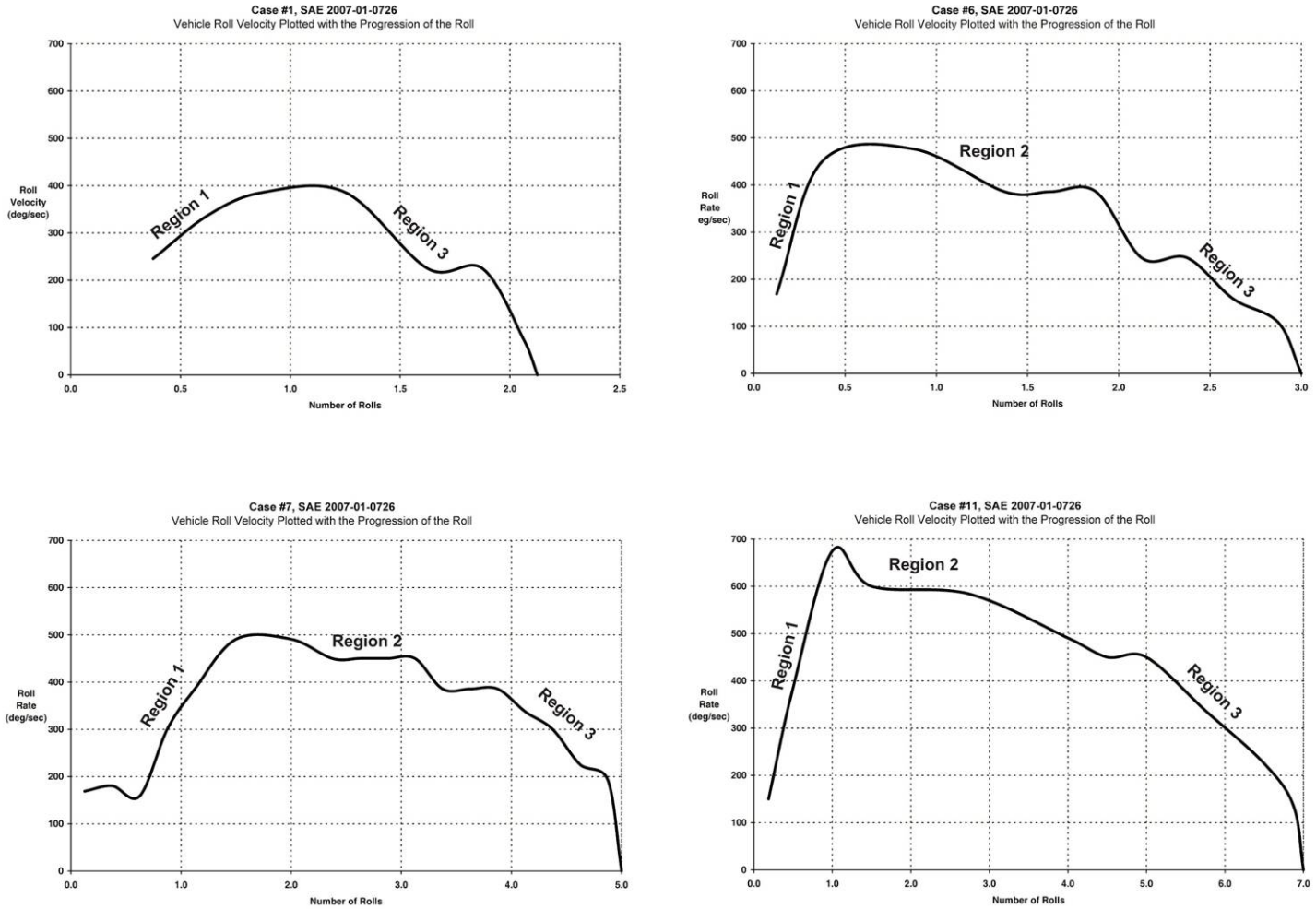

Figure 7

Downward Velocity

To establish a range of downward velocities that might occur during a rollover, begin by considering Figure 8.

Figure 8

This figure is a single frame from video of a rollover crash test run on the Controlled Rollover Impact System (CRIS) with a Ford Econoline van [8, *Image used with permission*]. The van in this test rolled six times, achieving roll velocities exceeding 600 degrees per second. In Figure 8, the van's CoM is elevated 5 to 6 feet above the ground. When this van begins to fall back to the ground from this elevated position, it will acquire a downward velocity that will be determined by the distance that its CoM falls. The following equation relates the distance the vehicle's CoM falls to its downward velocity at the end of that fall:

$$v_z = \sqrt{2gh_{drop}} \tag{10}$$

In this equation, v_z is the downward CoM velocity and h_{drop} is the distance the vehicle CoM drops as the vehicle travels back towards the ground. From the position depicted in Figure 8, the CoM of this van could realistically fall 3 feet before it impacts the ground again.

In this case, it would impact the ground with a downward CoM velocity around 9-½ mph. Given that the overall dynamics of this crash test are similar to the overall characteristics of many high-speed rollovers, downward velocities of this magnitude likely also occur during high-speed, real-world rollovers.

Figure 9 is a single frame from video of a vehicle in a rally race that exited the left edge of the roadway in a clockwise yaw (Case #4, SAE 2007-01-0726). The vehicle then impacted a ditch that ran perpendicular to the roadway and tripped with its driver's side leading. This ditch impact vaulted the vehicle into the air where it completed 2-¾ rolls before returning to the ground. The vehicle went on to roll an additional 1-¼ times (4 total rolls) and came to rest on its wheels. In the image above, the CoM of the vehicle is around 12 feet above the ground surface. Given this vault height, this vehicle would have a downward velocity around 19 mph when it reaches the ground again. This is an extreme case with a vault height that is likely rare. Nonetheless, this case does reveal that very high downward velocities can occur during rollovers.

Figure 9

The authors have elsewhere reported video analysis of a dolly rollover crash test [27] and analysis of three vehicle-to-ground impacts that occurred during that crash test [26]. In that test, the downward velocity for the three vehicle-to-ground impacts that were analyzed varied between 2.0 and 4.0 mph. Within Equations (1) through (9), the CoM downward velocity, v_{zi}, has direct and predictable effects, which are revealed explicitly by Equations (1) and (4). As the downward CoM velocity increases, so does the downward velocity at the vehicle-to-ground impact point ($v_{zc,i}$). As this downward velocity at the contact point increases, so does the vertical velocity change resulting from that impact. Given this relatively straightforward effect of the downward velocity, the parameter study presented later utilized only two values for the downward CoM velocity (2 and 4 mph). These are likely typical values for many dolly rollover crashes, but they are also clearly conservative assumptions in terms of what may be achieved during some real-world rollovers. Higher downward velocities would result in higher velocity changes than those presented in the parameter study.

Radius of Gyration and Vehicle Geometry

Having established reasonable ranges for the vehicle velocity conditions, a vehicle parameter set representing a typical mid-size to large sport utility vehicle was established. This parameter set was generated using inertial parameter data from the research and development website of the National Highway Traffic Safety Administration (NHTSA, http://www-nrd.nhtsa.dot.gov/vrtc/ca/rollover.htm). To use this data, the authors first excluded vehicles for which NHTSA had not reported both a CoM height and a roll moment of inertia. This left 409 entries. These 409 entries were sorted by vehicle type and then pickups, vans, and passenger cars were excluded. This left 128 sport utility vehicles. Finally, sport utility vehicles with weights below 3,200 pounds were eliminated.[2] This left 99 entries. The authors analyzed the inertial parameters for the remaining entries and established the following vehicle parameter set for this parameter study:

Vehicle Parameter Set (SUV)

- Vehicle Weight = 4,250 lb
- Roll Moment of Inertia = 550 lb-ft-sec^2
- Radius of Gyration = 2.04 ft
- Track Width = 62.0 inches
- CoM Height = 27.5 inches
- Roof Height = 68 inches

This parameter set represents roughly the average value of each parameter from the 99 entries for mid-size and large SUVs.[3] Of the six parameters listed, only the radius of gyration appears explicitly in Equations (1) through (9). Of course, the radius of gyration is calculated directly from the first two parameters, the vehicle weight and the roll moment of inertia. The last three parameters on the list – the track width, CoM height, and roof height – are used below, in conjunction with geometric relationships, to develop ranges for the impact radius and impact angle.

To determine the degree to which the radius of gyration influences the outcome of a vehicle-to-ground impact, it was first necessary to explore the degree to which this parameter might vary. Thus, after establishing the representative vehicle parameter set above, the authors calculated the standard deviation for the radius of gyration for the 99 mid-size and large SUVs. The standard deviation of the radius of gyration was 0.13

[2] This cutoff is somewhat arbitrary, but it did appear to eliminate most small SUVs. The goal here was not a rigorous statistical analysis, but simply a representative parameter set for mid-size to large SUVs.
[3] The average values were rounded to simplify the parameter set.

feet. Thus, the radius of gyration for nearly 95 percent of these SUVs fell within the range of 1.8 and 2.3 feet.

Impact Radius and Impact Angle

Having established a set of velocity conditions and a vehicle parameter set for our parameter study, next consider the range of impact angles that might be encountered during a rollover. To establish a range of impact angles, consider the Figure 10, which depicts the following four types of impacts that occur during rollovers: (1) leading side roof impacts, (2) trailing side roof impacts, (3) trailing side wheel impacts, and (4) leading side wheel impacts.

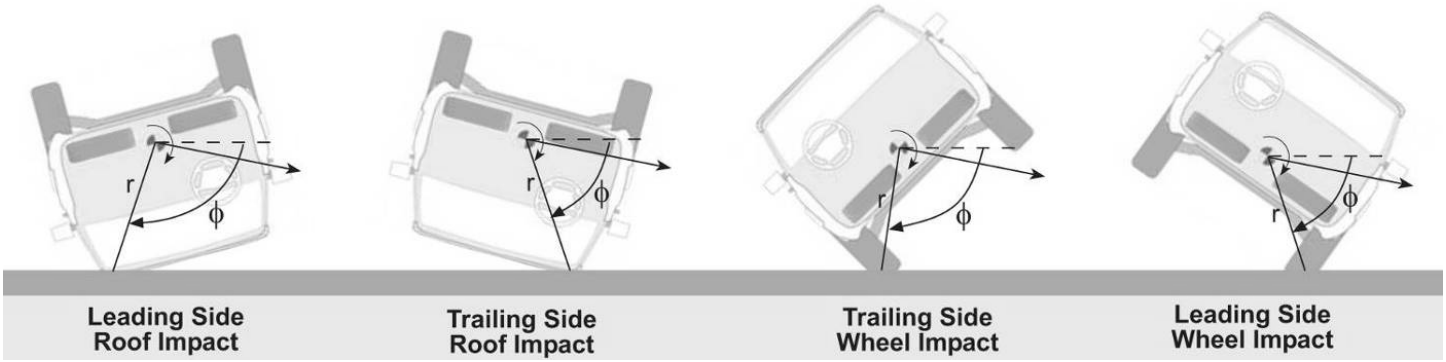

Figure 10

For each of these impact types, analytical expressions can be derived that will provide the maximum impact radius for that impact type based on the vehicle geometry. These expressions are listed below. In these equations, H is the overall vehicle height, h is the center of gravity height, w_{roof} is the roof width, and T is the track width.

The following equation gives the maximum impact radius for a roof-to-ground impact:

$$r_{roof,\max} = \sqrt{(H-h)^2 + \left(\frac{w_{roof}}{2}\right)^2} \qquad (11)$$

For now, assume that the roof width is approximately equal to the track width. For the vehicle used in the graphics of this paper, this assumption is reasonably accurate, but it will not necessarily be accurate for any particular vehicle. With this assumption and the hypothetical vehicle parameter set described above, this equation yields a value of 4.3 feet. The next equation below gives the maximum impact radius for a wheel-to-ground impact.

$$r_{wheel,\max} = \sqrt{h^2 + \left(\frac{T}{2}\right)^2} \qquad (12)$$

For the vehicle parameter set established above, this equation yields a value of 3.5 feet. Since vehicle deformation will act to reduce the impact radius that is realized during an impact with the ground, the parameter study that follows will not use these maximum values for the impact radius. Instead, the parameter study employs a range for the impact radius between 2.5 and 3.5 feet.

A reasonable range of impact angles for the vehicle geometry depicted in the above graphic was determined graphically, by orienting the vehicles at their minimum and maximum roll angles for each impact type and measuring the impact angle that would be associated with that orientation (assuming little to no deformation).[4] This process resulted in a range of impact angles between 55 and 135 degrees. This range of impact angles is defined based on geometric considerations. For impact angles that exceed 90 degrees, it is possible for the vertical velocity at the contact point to become positive. When this velocity becomes positive, an impact will not occur, even if the vehicle geometry allows it. The vertical velocity at the contact point will become positive when the impact angle is greater than 90 degrees and the following condition is met:

$$|v_{zi}| < |r \cdot \omega_{r,i} \cdot c\phi| \qquad (13)$$

Figure 11 plots the vertical velocity at the contact point for a range of impact angles between 55 and 135 degrees and a range of roll velocities between 200 and 600 degrees per second with a downward velocity of 2 mph. This graph reveals that for any impact angle greater than 105, the vertical velocity at the contact point will be positive and no impact will occur. Thus, while geometric considerations yield a range of impact angles between 55 and 135 degrees, the dynamic criteria of Equation (13) results in a narrower range between 55 and 105 degrees.

[4] Assuming little to no deformation at this point yields the largest range of impact angles.

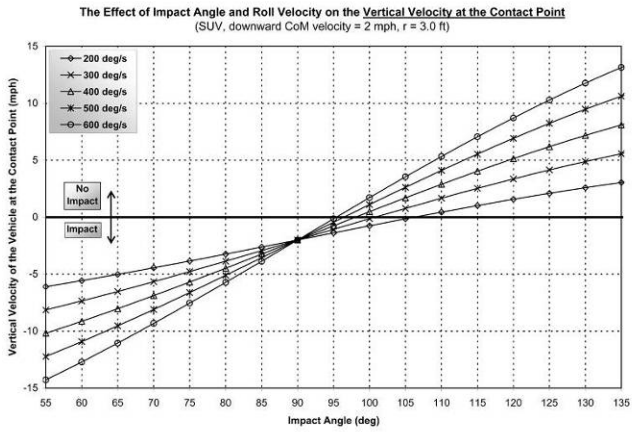

Figure 11

Another dynamic condition that needs to be considered is the requirement that the vertical velocity change that occurs as a result of a vehicle-to-ground impact must equal or exceed the vehicle's initial downward center-of-mass velocity. An impact will not be terminated until this condition is met. This ends up being a more restrictive dynamic criterion than the first, and as it turns out, this condition will not be met for any impact angle that exceeds 90 degrees. Thus, in the parameter study that follows, a range of impact angle between 55 and 90 degrees was used.[5]

Impact Duration

The duration of vehicle-to-ground contacts could potentially vary widely and would depend on many factors such as the features and stiffness of the surface on which the vehicle is rolling, the vehicle's translational speed and roll velocity, and the vehicle's shape and structural stiffness. Exploring and explaining the degree to which each of these factors influence the duration of vehicle-to-ground impacts is beyond the scope of the research reported in this paper. Here, we will only begin to scratch the surface and will take it only far enough to set a reasonable impact duration value for our parameter study.

To do this, consider NHTSA Test #3635, an FMVSS 208 dolly rollover test of a 1994 Ford Explorer run on a concrete test surface. As specified by FMVSS 208, the dolly used for this test had a speed of 30 mph before it was snubbed. The test vehicle was situated on the dolly such that the driver's side of the vehicle led into the roll with an initial roll angle of 23 degrees. During this test, the vehicle completed three rolls, coming to rest on its wheels. The vehicle was instrumented with 18 accelerometers, three angular rate sensors and four suspension displacement potentiometers. Two accelerometers recorded the longitudinal accelerations of the dolly. Eleven high-speed cameras, operating at approximately 250 frames per second, and one real-time camera captured the motion of the vehicle and the two unrestrained, 50th percentile ATDs that were in the vehicle during the test.

Figure 12 shows the resultant CoM acceleration for the vehicle in this test plotted with the progression of the three rolls that occurred. To generate this plot, the CoM accelerometer signals from each of the three vehicle-fixed coordinate directions were first filtered in accordance with SAE J211. Then, these signals were combined to obtain the magnitude of the resultant acceleration. The resulting signal retained a considerable amount of noise, so the signal was further smoothed using a 20-point moving average. These accelerations were then plotted with the progression of the roll by integrating the roll rate sensor data to determine the vehicle roll angle throughout the test. As this graph shows (Figure 13), integration of the roll rate sensor data resulted in about an eighth of a roll too little, indicating the sensor data has some inaccuracy. Nonetheless, Figure 13 is adequate to identify distinct acceleration pulses and to determine how these pulses should be synced with the roll motion of the vehicle. In this graph, eleven relatively distinct impacts have been identified with numeric labels.

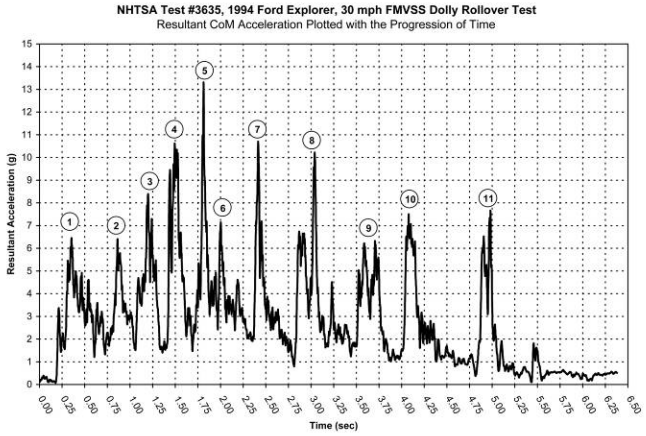

Figure 12

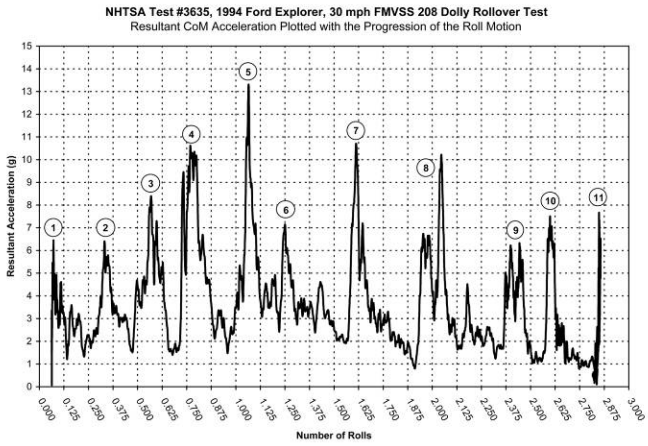

Figure 13

[5] This range of impact angles is applicable to the passenger's side leading roll used in the figures of this paper. For a driver's side leading roll with the same coordinate system, the relevant range of angles would be 90 to 125 degrees.

These same eleven impacts are identified in the second graph below and to the right, which shows the vehicle's resultant CoM accelerations plotted with the progression of time. Table 2 gives a description of the type of impact corresponding to each of these acceleration pulses and gives the approximate duration associated with each impact.

Impact Number	Description	Approximate Impact Duration (msec)
1	First Wheel Touchdown Following Vehicle Exit from Dolly	500
2	First Roof Impact (Leading Side)	335
3	Trailing Side Roof Impact	290
4	Trailing Side Wheel Impact	285
5	Leading Side Wheel Impact	410
6	Leading Side Roof Impact	
7	Trailing Side Roof Impact	450
8	Leading Side Wheel Impact	370
9	Leading Side Roof Impact	400
10	Trailing Side Roof Impact	215
11	Wheel Impact	250

TABLE 2

These impact durations vary between 200 and 500 milliseconds. The authors have elsewhere presented video analysis of another dolly rollover crash test run with a sport utility vehicle on a concrete surface along with analysis of three vehicle-to-ground impacts that occurred during that crash test [26, 27]. In that test, the impact durations for the three vehicle-to-ground impacts that were analyzed varied between 165 and 230 milliseconds when obtained with the vehicle accelerations. Thus, between these two tests, the impact durations varied between 165 and 500 milliseconds. For the purpose of our parameter study, we chose an impact duration of 300 milliseconds, a value lying towards the middle of this range.

Coefficient of Restitution and Impulse Ratio

In theory, one could examine rollover crash test data to determine reasonable ranges for the coefficient of restitution and the impulse ratio. This would involve analyzing sensor data and video footage to obtain quantitative data about the vehicle dynamics and then fitting an impulse-momentum impact model solution to each of the vehicle-to-ground impacts that occurred during the test [24]. Using sensor data to conduct such analysis would have considerable challenges associated with it. First of all, the authors have encountered few, if any, rollover crash tests that utilize sufficient instrumentation to completely resolve the three-dimensional dynamics of the test vehicle. Even if one had a test with sufficient sensor data, analyzing this data over the multiple-second time periods typically associated with rollover tests must contend with noise in the sensor signals, potential sensor position and alignment errors, and uncertainties that accrue during numerical integration [27].

For the purpose of the current study, the authors chose to simply set the coefficient of restitution to a value of zero. Based on research related to restitution for other impact types [23], our expectation would be for the coefficient of restitution for a vehicle-to-ground impact to vary with the impact conditions and the structural properties of the vehicle and the ground. Nonetheless, in Equations (1) through (9), the coefficient of restitution only appears explicitly in Equation (1) and within that equation it has a direct and predictable effect on the result. Namely, the coefficient of restitution gets added to 1 and acts as a multiplier that increases the value of the vertical velocity change. A coefficient of restitution of 0.1 increases the vertical velocity change 10%; a coefficient of restitution of 0.2 increases the vertical velocity change by 20%, and so forth. Since our primary goal within this study is to understand principles and trends surrounding how vehicle-to-ground impact conditions influence the rollover dynamics and since the coefficient of restitution influences these dynamics in a predictable manner, we judged that its value could be set to zero without obscuring the behavior of Equations (1) through (9).

As far as the impulse ratio goes, it was assumed that the ground surface impact force develops entirely due to sliding between the vehicle and the ground (no snagging or furrowing) and that a coefficient of friction of 0.5 would reasonably represent the available friction for a vehicle body sliding on the ground. As has already been stated, the appropriateness of treating the impulse ratio as a coulomb friction value in this way depends on the situation. The most rigorous way of viewing the impulse ratio is simply to see it as the ratio of the ground surface and vertical impulses. If the ground plane force is generated entirely by sliding, then the analogy to a friction coefficient is appropriate. However, it should be observed at this point that for any particular vehicle-to-ground impact, there is a critical value of the impulse ratio, μ_c, that will cause relative motion between the vehicle and the ground to cease in the contact region. The impulse ratio should not be set at a value that exceeds this critical impulse ratio since this will result in physically unrealistic results.

For any given impact scenario, the relative magnitude of the available friction coefficient to the critical impulse ratio will have physical significance. The available friction coefficient represents the magnitude of friction force that can be recruited during the impact. The critical impulse ratio represents the magnitude of friction force that must be recruited in order for relative motion to cease along the ground surface in the contact region between the vehicle and the ground. When the critical impulse ratio is greater than the available friction coefficient, then all of the available friction will be recruited during the impact, but that friction will be insufficient to cause sliding to cease in the contact region. When the available friction coefficient exceeds the critical impulse ratio, only a portion of the available friction will be recruited and sliding will cease in the contact region. In such cases, the value of the impulse ratio for the impact model

should be set at the value of the critical impulse ratio, not the available friction coefficient. This is because recruitment of the available friction depends on relative velocity being present between the ground and the vehicle body. Once this relative motion ceases, no additional friction can be recruited.

In terms of the symbols used within the impact model that is the subject of this paper, the critical impulse ratio for any particular vehicle-to-ground impact is the value of the impulse ratio that results in the final velocity at the Point C being zero, as follows:

$$v_{yc,f} = v_{y,f} + r \cdot s\phi \cdot \omega_{r,f} = 0 \qquad (14)$$

The critical impulse ratio will depend on the vehicle mass and rotational inertia, the impact radius and impact angle, the coefficient of restitution, the impact duration and the velocity conditions. To illustrate how the critical impulse ratio is influenced by some of these parameters, the authors calculated the critical impulse ratio for the following parameter set:

Translational Speed = 10 to 40 mph
Downward Velocity = 2 mph
Roll Velocity = 200 to 600 deg/sec
e = 0
r = 3 ft
Δt = 300ms
Impact Angle = 55 to 90 deg

The critical impulse ratio for these impact conditions are plotted in the four graphs of Figure 14. In these graphs, the impact angle is plotted on the horizontal axis and the impulse ratio on the vertical axis. Each graph contains a curve for roll velocities of 200, 300, 400, 500 and 600 degrees per second. The first graph is for a translational speed of 40 mph, the second 30 mph, the third 20 mph and, the last, 10 mph. The dark horizontal lines on each graph mark the upper (positive) and lower (negative) friction limits. Any impact scenario that lies between these dark lines has a critical impulse ratio less than the available friction coefficient.

From these graphs, the following observations can be made:

- When the translational speed is 40 mph, all of the impact scenarios represented in the graph have critical impulse ratios that exceed the available friction coefficient. Thus, for these impacts, the impulse ratio would take on the value of the available friction.

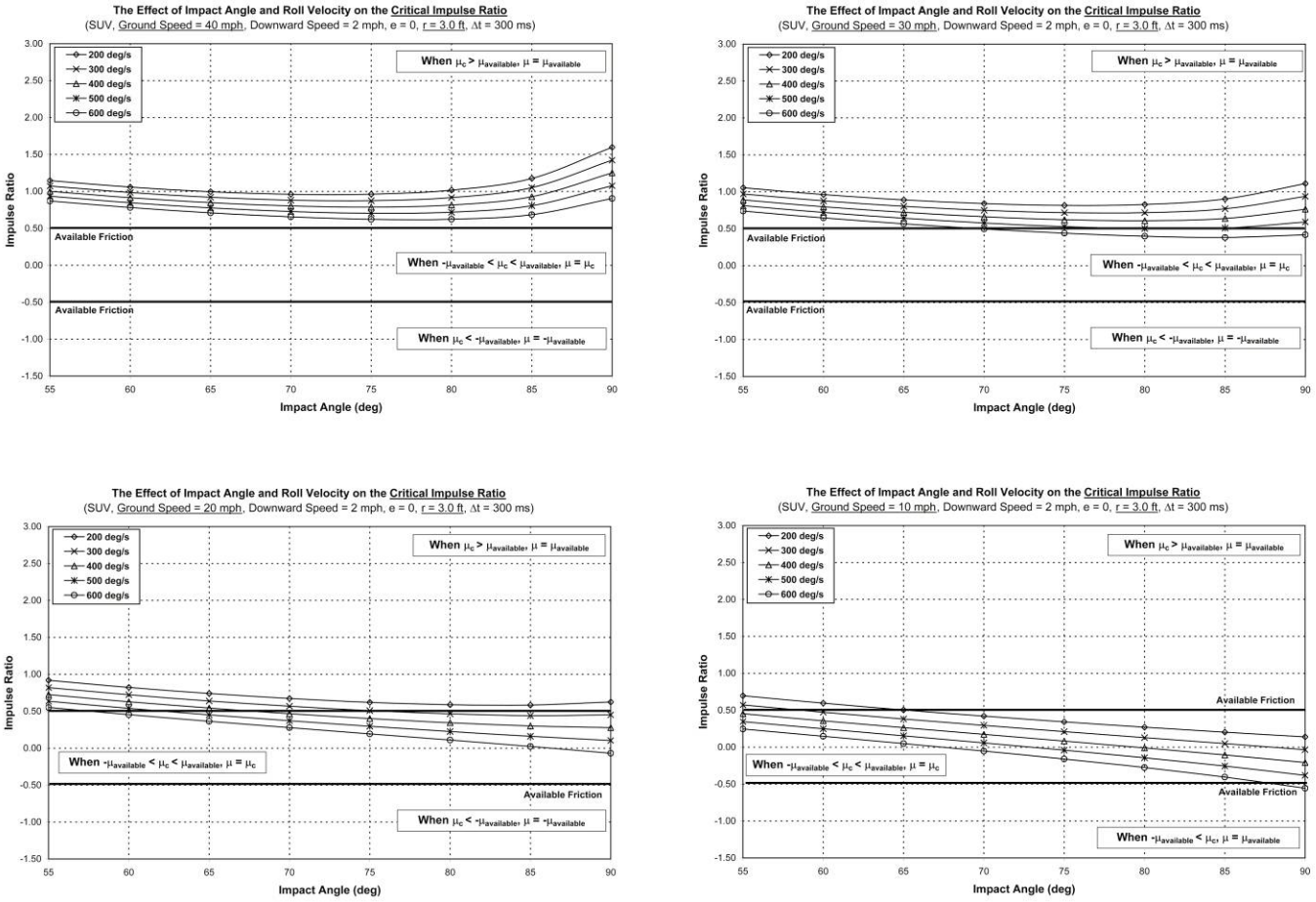

Figure 14

- When the translational speed drops to 30 mph, most of the impact scenarios still have critical impulse ratios that exceed the available friction coefficient. However, a portion of the 500 and 600 deg/sec curves have begun to dip below the available friction line. When this occurs, the impulse ratio will take on the value of the critical impulse ratio.

- When the translational speed drops to 20 mph, none of the curves remain entirely above the available friction line. Roll velocities between 200 and 600 deg/sec produce numerous impact scenarios where the available friction is more than adequate to cause sliding to cease in the contact region between the vehicle body and the ground.

- When the translational speed drops to 10 mph, almost all of the impact scenarios have critical impulse ratios with a magnitude less than the available friction.

- At a translational speed of 10 mph, a number of impact scenarios have resulted in critical impulse ratios that are negative, but still below the available friction threshold. Physically, this corresponds to a situation where the ground plane component of the perimeter velocity has become greater than the ground plane CoM velocity and, therefore, a switch in direction of the ground plane impact force has occurred.

In general, these graphs demonstrate that as the translational speed decreases during a rollover, the critical impulse ratio becomes less and it becomes more likely that sliding will cease at the vehicle-ground interface during the impact.

PARAMETER STUDY RESULTS

The pages of Appendix B contain graphs showing the parameter study results, which are described in this section. The first six of these pages, identified with the designations A1, A2, A3, A4, A5 and A6 contain graphs depicting the CoM upward ΔV for a number of impact scenarios. The first of these pages, A1, contains four graphs, each produced with a CoM downward speed of 2 mph, a coefficient of restitution of zero, an impact radius of 3.0 feet, and an impact duration of 300 milliseconds. Within each graph, the impact angle has been varied between 55 and 90 degrees and the roll velocity between 200 and 600 degrees per second. Impact scenarios at varying translational speeds are depicted in the four graphs, with one graph utilizing a translational speed of 40 mph, the next 30 mph, the next 20 mph, and the last, 10 mph. The impact scenarios represented on Page A2 are identical to those on Page A1 with the exception that the impact radius has been reduced from 3.0 feet to 2.5 feet. Page A3 again represents impact scenarios identical to those on Page A1 with the exception that the impact radius has been increased to 3.5 feet. The graphs on Page A4 return to an impact radius of 3.0 feet, but the CoM downward velocity has been increased to 4 mph. Pages A5 and A6 again utilize an impact radius of 3.0 feet and a downward CoM speed of 2 mph, but the radius of gyration has been changed to 1.8 and 2.3 feet, respectively. Thus, the 24 graphs on Pages A1 through A6 enable examination of the influence of the translational speed, downward speed, roll velocity, impact angle, impact radius, and radius of gyration on the CoM upward ΔV for a range of vehicle-to-ground impacts.

Pages B1 through B4 contain graphs representing the CoM ground plane ΔV for the same impact scenarios represented in the graphs of Pages A1 through A4. Pages C1 through C6 contain graphs representing the change in roll velocity for the same impact scenarios represented in Pages A1 through A6. Page D4 contains graphs representing the change in vertical velocity at the vehicle-to-ground contact point for the impact scenarios with a CoM downward speed of 4 mph and an impact radius of 3.0 feet. Page E1 contains graphs representing the energy loss for the impact scenarios represented on Pages A1, B1 and C1. This section summarizes the trends that are exhibited by each of these plots, and then, the physical meaning of these trends is drawn out in the “Discussion” section.

Vertical CoM ΔV

TRANSLATIONAL SPEED: The degree to which the translational speed influenced the magnitude of the vertical velocity change was governed by the critical impulse ratio and the available friction limit. As long as the critical impulse ratio exceeded the available friction limit, the vertical velocity change was maximized and changing the translational speed did not influence the vertical velocity change. When the translational speed became low enough that the critical impulse ratio became less than the available friction coefficient, the vertical ΔV would drop to a lower level. Then, when the ground surface component of the rotational perimeter velocity exceeded the CoM translational speed, the impulse ratio would become negative and the vertical ΔVs would again drop to a lower magnitude. Physically, this means that the translational speed at the contact point, which is determined by both the CoM translational speed and the roll velocity, influences the magnitude of the vertical velocity change. The highest vertical velocity changes occur when the translational speed is the highest (assuming a fixed downward velocity).

ROLL VELOCITY: The vertical velocity change increased as the roll velocity increased. The magnitude of this roll velocity effect depended on the impact angle, with roll velocity differences having the greatest effect at the lowest impact angles. As the impact angle increased up to 90 degrees, the effect of roll velocity on the vertical velocity change diminished and ultimately disappeared

(at 90 degrees). The magnitude of the roll velocity effect was also influenced by the translational speed with the roll velocity making the largest difference at the higher translational speeds.

IMPACT ANGLE: The vertical velocity change was influenced nonlinearly by the impact angle. The magnitude and character of this influence was determined by the magnitude of the critical impulse ratio relative to the available friction coefficient, and thus, was affected by the translational speed, the roll velocity, and the impact radius. At an impact angle of 90 degrees, the velocity change was independent of the translational speed, the roll velocity, the impact angle and the impact radius and was numerically equal to the initial downward velocity of the CoM (when e=0).

IMPACT RADIUS: The vertical ΔVs increased as the impact radius increased. The impact radius also influenced the nature of the relationship between the impact angle and the upward CoM velocity change.

DOWNWARD SPEED: Increasing the downward speed had the effect of increasing the vertical ΔVs in the predictable manner one would expect from Equations (1) and (4). None of the previously observed patterns were altered by the increase in downward velocity. It should be noted, however, that changing the magnitude of the downward velocity did influence the magnitude of the critical impulse ratio, and therefore, would affect where each of these patterns shows itself.

RADIUS OF GYRATION: Increasing the radius of gyration, from 1.8 feet to 2.04 feet, and then, from 2.04 feet to 2.3 feet, had the effect of flattening the upward CoM ΔV curves and of changing the impact angle at which the maximum ΔV occurred. The overall effect was that the ΔVs at some impact angles increased, while at others they decreased.

Ground Plane CoM ΔV

TRANSLATIONAL SPEED: As with the vertical velocity change, it can be observed that the degree to which the translational speed influenced the magnitude of the translational surface ΔV was governed by the critical impulse ratio and the available friction limit. In the case of the ground surface ΔV, though, this influence is more pronounced due to the additional multiplication by the impulse ratio. Overall, as the magnitude of the translational speed diminished, so did the magnitude of the ground plane velocity change. In fact, when the translational speed was at 10 mph, a number of impact scenarios resulted in negative ground plane velocity changes (increases in the translational speed). Since the accumulation of the ground plane velocity changes during a rollover will determine the rate at which the vehicle will decelerate, this trend seems to indicate that the overall deceleration rate experienced by a vehicle during a rollover would depend on the initial translational speed, with higher deceleration rates being associated with higher initial translational speeds. Of course, other factors also influence the ground surface ΔV, and so, additional study would be necessary to determine the degree to which this trend in the ground surface ΔV would play out over the course of an entire roll sequence.

ROLL VELOCITY: As long as the critical impulse ratio remained above the available friction coefficient, higher roll velocities produced higher ground surface ΔVs than did lower roll velocities. Once the critical impulse ratio began dropping below the available friction coefficient, the ground surface ΔVs began dropping in magnitude. Ultimately, as the translational speed dropped and more and more impact scenarios had impulse ratios that fell within the friction limits, a new trend was established where the higher roll velocities produced lower ΔVs than the lower roll velocities.

IMPACT RADIUS: Higher impact radii produced higher ground surface ΔVs. Also, the higher the impact radius, the sooner (in terms of translational speed) the critical impulse ratio became less than the available friction coefficient.

DOWNWARD SPEED: Increasing the downward speed increased the ground surface velocity change.

Change in Roll Velocity

TRANSLATIONAL SPEED: At the higher translational speeds, most of the impact scenarios resulted in increases in roll velocity. As the translational speed dropped and the critical impulse ratios began to drop below the available friction coefficient, the shape of the curves for the change in roll velocity began to change and the magnitude of the changes began to drop. Ultimately, as the translational speed continued to drop, an increasing number of impact scenarios began to result in decreases in roll velocity. At a translational speed of 10 mph, most of the impact scenarios resulted in a decrease in roll velocity.

ROLL VELOCITY: At higher translational speeds, the initial roll velocity had a noticeable, but nonetheless small, effect on the magnitude of the change in roll velocity. As the translational speed decreased, the initial roll velocity became much more influential in determining the change in roll velocity, with the highest roll velocities producing the highest decreases in roll velocity.

IMPACT ANGLE: At higher translational speeds, the highest increases in roll velocity were at the highest impact angles. The lowest impact angles produced decreases in roll velocity even at the higher translational speeds. At lower translational speeds, the lowest impact angles produced the highest magnitude decreases in roll velocity, although the influence of the impact angle was

much less pronounced than it was at the higher translational speeds.

IMPACT RADIUS: At the higher translational speeds, increasing the impact radius increased the magnitude of the change in roll velocity that was realized for any given impact scenario. Increasing the impact radius also increased the rate at which the changes in roll velocity transitioned into the negative region (when viewed as a function of translational speed). Once the transition into the negative region had occurred, increasing the impact radius again increased the magnitude of the change in roll velocity that was realized for any given impact scenario.

DOWNWARD VELOCITY: Changing the downward CoM speed had a relatively small effect on the change in roll velocity that a particular impact scenario produced.

RADIUS OF GYRATION: At high translational speeds, the radius of gyration had a relatively significant effect on the change in roll velocity that occurred during a vehicle-to-ground impact. Specifically, a higher radius of gyration yielded a lower change in roll velocity. At lower translational speeds, the radius of gyration had a much less significant effect.

Vertical ΔV at the Contact

TRANSLATIONAL SPEED: The vertical ΔV of the vehicle in the contact region depended directly on the vertical ΔV of the vehicle at the CoM and on the vehicle's change in roll velocity. Interestingly, though, the vertical ΔV in the contact region showed no dependence on the translational speed.

ROLL VELOCITY: Higher roll velocities resulted in higher contact region upward velocity changes. The only exception to this was at an impact angle of 90 degrees, where the contact region upward ΔV was independent of the roll velocity.

IMPACT ANGLE: The contact region upward ΔV was the highest at the lowest impact angles and decreased linearly with increasing impact angle. The roll velocity effects were the greatest at low impact angles and decreased as the impact angle increased.

Energy Loss

TRANSLATIONAL SPEED: The energy loss associated with a particular impact was the highest when the translational speed was the highest and diminished as the translational speed diminished.

ROLL VELOCITY: Roll velocity had a definite influence on the energy loss associated with an impact. However, the nature of that relationship depended heavily on the impact angle.

IMPACT ANGLE: The energy loss associated with a particular impact tended to decrease as the impact angle increased.

DISCUSSION

This paper has explored the influence of vehicle-to-ground impact conditions on the dynamics and the severity of rollover crashes. The equations of an impulse-momentum vehicle-to-ground impact model were used to explore the ways in which and the extent to which rollover dynamics and severity are influenced by the following factors: (1) the vehicle's shape and its orientation at impact [represented by the impact angle and radius], (2) its weight, center-of-mass location, and roll moment of inertia [represented by the vehicles radius of gyration and the impact angle and radius], (3) its translational speed, (4) its downward velocity, and (5) its roll velocity. From this parameter study, several observations can be made.

The Effects of Translational Speed

First, a high initial translational speed is a factor that contributes to causing multiple rolls and the characteristic three-region shape of the roll velocity curves presented earlier. To see physically why this is the case, consider again the following equation, which yields the change in roll velocity for a vehicle-to-ground impact:

$$\Delta\omega_r = \left(\Delta V_z + g \cdot \Delta t_i\right) \cdot \frac{r \cdot \left(\mu \cdot s\phi - c\phi\right)}{k_r^2} \qquad (15)$$

All of the terms in this equation will always be positive, with the exception of the $\mu \cdot s\phi - c\phi$ term. That being the case, the sign of this term will determine the sign of the change in roll velocity and, thus, whether the roll velocity will increase or decrease. To see the physical meaning of this $\mu \cdot s\phi - c\phi$ term, consider again the idealized vehicle-to-ground impact depicted in Figure 15.

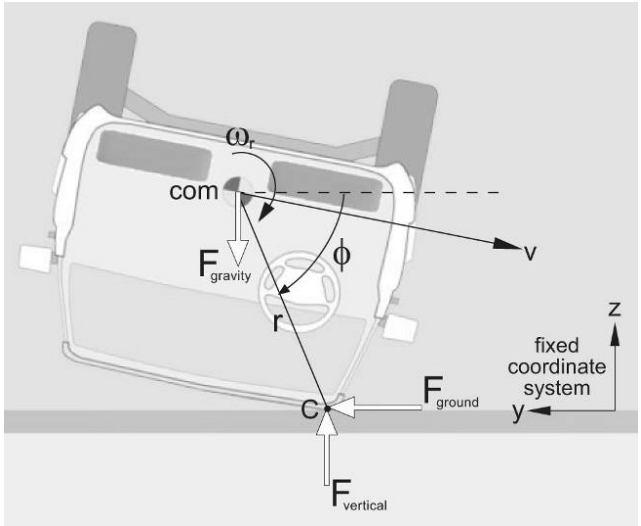

Figure 15

As this figure shows, during a vehicle-to-ground impact, there are three forces applied to the vehicle – the force of gravity (the vehicle weight) and the ground surface and vertical components of the impact force. It is the moments applied to the vehicle by the components of the impact force that determine whether the roll will be accelerated or decelerated as a result of the impact.

When the right side of Equation (16) is positive, the roll velocity will increase and, when it is negative, the roll velocity will decrease. Thus, the roll will be accelerated when

$$F_{ground} \cdot r \cdot s\phi - F_{vertical} \cdot r \cdot c\phi > 0 \qquad (17)$$

Multiplying Equation (17) by the impact duration (Δt_i), then recognizing that $F_{ground} \cdot \Delta t_i = m\Delta V_y$ and that $F_{vertical} \cdot \Delta t_i = m\Delta V_z$, and that $\Delta V_y = \mu \Delta V_z$, yields the following sequence of equations:

$$\begin{aligned} &\frac{F_{ground} \cdot \Delta t_i}{F_{vertical} \cdot \Delta t_i} \cdot s\phi - c\phi \\ &= \frac{\Delta V_y}{\Delta V_z} \cdot s\phi - c\phi \\ &= \frac{\mu \Delta V_z}{\Delta V_z} \cdot s\phi - c\phi > 0 \end{aligned} \qquad (18)$$

The last equation in this sequence can be simplified to yield the following condition under which a vehicle-to-ground impact will yield an increase in roll velocity:

$$\mu \cdot s\phi - c\phi > 0 \qquad (19)$$

The condition of Equation (19) is equivalent to the sign controlling term of Equation (15). Thus, this condition relates physically to the balance of moments applied to the vehicle by the impact force components.

Figure 16 shows the effect of the impulse ratio, μ, and the impact angle, ϕ, on the value of this $\mu \cdot s\phi - c\phi$ term. The impulse ratio is plotted on the horizontal axis of this graph and the graph contains a curve for four different impact angles – 55, 65, 75 and 85 degrees. The magnitude of the $\mu \cdot s\phi - c\phi$ term is plotted on the vertical axis. For an impulse ratio of 0.5, impact angles of 65, 75 and 85 degrees all resulted in a positive value for this term (roll velocity increases). Only an impact angle of 55 degrees resulted in a negative value for this term (roll velocity decrease). As the impulse ratio decreases from 0.5, the maximum impact angle for which the $\mu \cdot s\phi - c\phi$ term yields a negative value increases. By the time the impulse ratio reaches zero, all of the impact angles result in a negative value for the $\mu \cdot s\phi - c\phi$ term, and thus, they all result in roll velocity decreases.

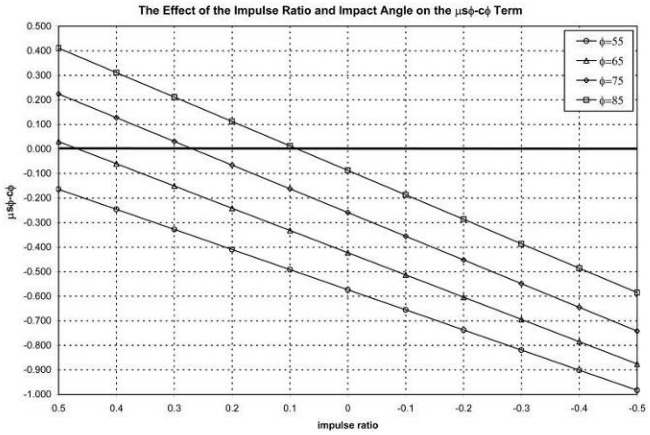

Figure 16

Now, recall that the impulse ratio is determined, first, by the ground plane velocity of the vehicle at the vehicle-to-ground interface and, second, by the available friction. At higher translational speeds, the critical impulse ratio exceeds the available friction for all of the impact scenarios in the parameter study, and thus, the impulse ratio takes on the value of the available friction (0.5, in this case). At this impulse ratio, most possible impact scenarios result in an increase in roll velocity. Thus, at higher translational speeds, where the impulse ratio takes on the available friction value, the roll will tend to be accelerated. As the translational speed of the vehicle diminishes, the ground plane velocity of the vehicle at the vehicle-to-ground interface diminishes to the point where the critical impulse ratios fall below the magnitude of the available friction coefficient and, in some cases, become negative. When this occurs, the impulse ratio takes on the value of the critical impulse ratio and an increasing number of impact scenarios result in decreases in roll velocity. The lower the vehicle's translational speed, the higher the decreases in roll velocity can be and the more likely it becomes that the roll will be terminated. Thus, at high translational speeds, roll velocity increases are likely; at mid-range translational speeds, low magnitude increases or decreases are likely; and at low translational speeds, high magnitude decreases in roll velocity become likely. This is the pattern that shows up in the three-region behavior of the roll velocity curves reported earlier.

The parameter study also yields the observation that a high initial translational speed is a factor that adds severity to vehicle-to-ground impacts. That is, holding all other impact conditions fixed, the impacts at the higher translational speeds will be more severe than those at lower translational speeds. This can be seen in the parameter study graphs in Appendix B, which show the vertical and ground plane velocity changes. The higher translational speeds consistently produce higher magnitude velocity changes – and therefore higher impact forces – than the lower translational speeds.[6]

[6] This point in the discussion is also an ideal point to observe that one of our conclusions in Ref. 25 was incomplete. Specifically, that

The Deceleration Rate for a Rolling Vehicle

Next, it can be observed that the rate at which a rolling vehicle decelerates will be determined by the accumulation of the ground plane velocity changes that occur during the rollover. Thus, any factor that influences the ground surface velocity changes will also influence the deceleration rate that the vehicle experiences. These factors include the following: (1) the available surface friction, (2) the translational speeds, vertical velocities, and roll velocities experienced during the roll, (3) the orientations of the specific vehicle-to-ground impacts that occur during the roll, (4) the vehicle geometry, (5) and the stiffness of the vehicle structures engaged during the roll. The degree to which each of these factors will influence the deceleration rate during a particular vehicle-to-ground impact could be explored by examining the following equation:

$$a_{y,avg} = \frac{\Delta V_y}{g\Delta t_i} = \frac{\mu}{\Delta t_i} \cdot \left(\Delta V_z + g\Delta t_i\right) \qquad (20)$$

This equation will yield the average ground plane deceleration rate during a vehicle-to-ground impact. The graphs of Figure 17 show how this average deceleration rate varies with translational speed, roll velocity, and impact angle. Inherent in these graphs is also the effect of changing impulse ratio values, which are determined by the translational speed of the vehicle in the contact region and the available friction.

As these graphs show, each of these factors does influence the average deceleration rate during the impact. Generally speaking, higher translational speeds produce impacts of higher deceleration rate. The roll velocity has an intriguing influence, with higher roll velocities producing higher deceleration rates at the higher translational speeds, but lower deceleration rates at the lower translational speeds. Ultimately, an empirical study of crash test data would be necessary to explore how each of these factors affects the deceleration rate over the course of an entire rollover.

No one has undertaken such a study to date, though Keifer [14] made the interesting suggestion that in the sixteen Malibu tests [1, 19], the average deceleration rate of the vehicles was inversely related to the number of rolls, with the highest deceleration rates occurring with the fewest number of rolls.

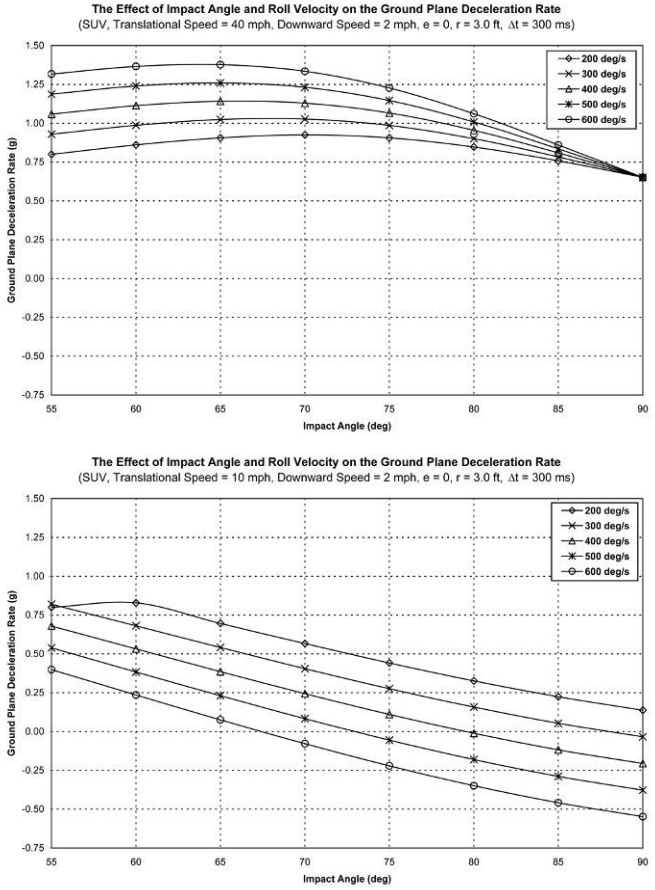

Figure 17

Figure 18 shows the deceleration rates for the sixteen Malibu tests plotted versus the number of rolls.[7] Visually, there does appear to be a downward trend in the deceleration rate with the number of rolls. However, there is considerable variability in the data and fitting a line to the data only yields a rather weak direct relationship between the number of rolls and the deceleration rate. Even in regard to the visual trend of the data toward decreasing deceleration rate with increasing number of rolls, it should be observed that the Malibu tests were run with vehicles of nearly identical external geometry, with the same nominal test conditions on the same test surface. Thus, these tests would not reveal the influence of surface friction, initial translational speed or variations in vehicle geometry on the deceleration rate. Most likely, any relationship that does exist between the number of rolls and the deceleration rate would only be valid for a single vehicle model with a single test setup with a single test surface and would reflect the variability in the roll velocities achieved by the test vehicles in each particular test.

conclusion stated: “Severe roof-to-ground impacts are associated with either significant increases or significant decreases in roll velocity.” If this statement is taken to say that significant changes in roll velocity constitute a severe event, then this statement may be true. However, if this statement is taken to imply that significant translational velocity changes are associated with significant increases or decreases in roll velocity, then from the parameter study results reported above, we must state that significant translational velocity changes can occur with or without significant changes in roll velocity.

[7] The deceleration rates plotted on this graph are different than those reported by Keifer.

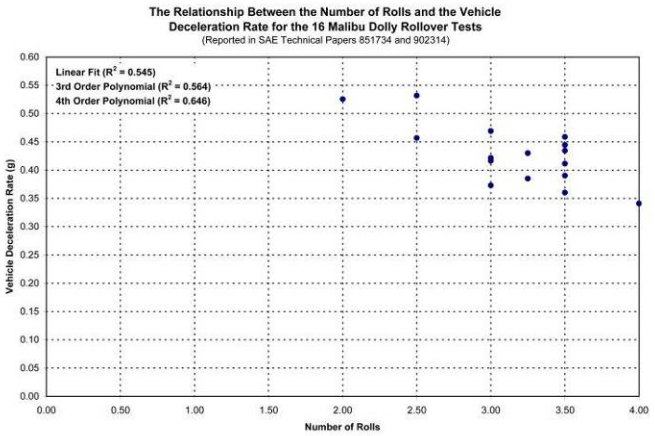

Figure 18

This is confirmed, at least preliminarily, by examining the results from two dolly rollover crash tests reported by Luepke [15]. These two tests involved SUVs rolling from speeds around 43 mph on desert soil. In these tests, the vehicle experienced 4 and 4-¼ rolls, and yet, exhibited deceleration rates of 0.52 and 0.53. These deceleration rates are in the same range as those for the Malibu tests that only experienced 2 to 2-½ rolls, so clearly any validity to the relationship observed by Keifer breaks down for different test conditions. A similar dolly rollover reported by Yamaguchi [28] shows a similar outcome (deceleration rate of 0.52) with similar test conditions (41.7 mph launch on desert soil). Similarly, Case #3 from SAE 2007-01-0726 discussed above exhibited a similar deceleration rate (0.53) for similar conditions (an SUV rolling on grass and dirt from an initial speed of 48 mph). That these deceleration rates are higher than those from the Malibu tests – and, for that matter, than most passenger car dolly rollovers on asphalt or concrete surfaces – is likely due to the differences in initial speeds, vehicle geometry and test surface. Future research could further explore Equation (18) along with test data to determine the degree to which each of these factors might affect a rolling vehicle's deceleration rate.

CONCLUSIONS

- A high initial translational speed (≈30+ mph) is a factor that contributes to causing multiple rolls and the characteristic three-region shape of a typical roll velocity curve.

- If all other impact conditions are held fixed, a vehicle-to-ground impact occurring at a high translational speed will be more severe than one occurring at a low ground speed.

- The rate at which a rolling vehicle decelerates will be determined by the accumulation of the ground plane velocity changes that occur during the rollover. Thus, the following factors will likely influence the rate a which a rolling vehicle decelerates: (1) the available surface friction, (2) the translational speeds, vertical velocities, and roll velocities experienced during the roll, (3) the orientations of the specific vehicle-to-ground impacts that occur during the roll, (4) the vehicle geometry, (5) and the stiffness of the vehicle structures engaged during the roll.

FURTHER RESEARCH

- The discussion in this paper demonstrates that the critical impulse ratio is an important concept for understanding rollover dynamics. That being the case, this concept deserves further attention. Brach and Brach [4] reported an analytical expression for the critical impulse ratio for a planar impulse-momentum impact model similar to the one employed in this paper. An equivalent expression for the impact model used in this paper could likely be derived and this expression could cast further light on the physical reasons for the existence of certain rollover crash attributes.

- In this paper, we have explored the influence that certain parameters have on the severity of vehicle to ground impacts. The vehicle parameter set, however, was limited to one applicable to mid-size to large sport utility vehicles. This study could be extended by using the impact model to explore other vehicle parameter sets. One question that this model could potentially address would be why vehicle aspect ratio influences injury rates in rollovers. Padmanaban, Moffatt and Marth [20] found that "low, wide vehicles have higher odds of fatality or serious injury" and that "the aspect ratio was the only vehicle parameter studied that had a pronounced effect in influencing the odds of fatality…Higher aspect ratio vehicle's were found to have fewer fatally injured drivers given that a rollover occurred." The impact model used in this paper could potentially be used to offer a causative explanation for this statistical conclusion.

REFERENCES

1. Bahling, G.S., et al., "Rollover and Drop Tests – The Influence of Roof Strength on Injury Mechanics Using Belted Dummies," SAE Technical Paper Number 902314.

2. Barrentine, Larry B., An Introduction to Design of Experiments: A Simplified Approach, American Society for Quality, 1999.

3. Brach, Raymond M., Mechanical Impact Dynamics: Rigid Body Collisions, 2007. This reference is available at www.brachengineering.com.

4. Brach, Raymond M., Brach, R. Matthew, Vehicle Accident Analysis and Reconstruction Methods, SAE, 2005.

5. Brach, Raymond M., Brach, R. Matthew, “A Review of Impact Models for Vehicle Collision,” SAE Technical Paper Number 870048.

6. Brach, Raymond M., Brach, R. Matthew, “Energy Loss in Vehicle Collision,” SAE Technical Paper Number 871993.

7. Brach, Raymond M., “An Impact Moment Coefficient for Vehicle Collision Analysis,” SAE Technical Paper Number 770014.

8. Carter, Jarrod W., et al., “A Comparison of the Controlled Rollover Impact System (CRIS) with the J2114 Rollover Dolly, SAE Technical Paper Number 2002-01-0694.

9. Chen, H. Fred, Guenther, Dennis A., “Modeling of Rollover Sequences,” SAE Technical Paper Number 931976.

10. Fonda, Albert G., “Nonconservation of Momentum During Impact,” SAE Technical Paper Number 950355.

11. Friedman, Donald, “Roof Crush Versus Occupant Injury From 1988 to 1992 Nass,” SAE Technical Paper Number 980210.

12. Funk, James, “Application of an Occupant Ejection Trajectory Model to Real-World Rollover Crashes,” forthcoming from SAE.

13. Hughes, Raymond J., et al., “A Dynamic Test Procedure for Evaluation of Tripped Rollover Crashes,” SAE Technical Paper Number 2002-01-0693.

14. Keifer, Orion P., “Vehicle Linear and Rotational Acceleration, Velocity and Displacement during Staged Rollover Collisions,” SAE Technical Paper Number 2007-01-0732.

15. Luepke, Peter, et al., “An Evaluation of Laminated Side Window Glass Performance During Rollover,” SAE Technical Paper Number 2007-01-0367.

16. Malliaris, C., “Pivotal Characterization of Car Rollovers,” Proceedings of the 13th ESV Conference, November 1991.

17. Marine, Micky C., “On the Concept of Inter-Vehicle Friction and Its Application in Automobile Accident Reconstruction,” SAE Technical Paper Number 2007-01-0744.

18. Mills, P.J., Hobbs, C.A., “The Probability of Injury to Car Occupants in Frontal and Side Impacts,” SAE Technical Paper Number 841652.

19. Orlowski, K. Bundorf, R.T., Moffatt, E.A., “Rollover Crash Tests – The Influence of Roof Strength on Injury Mechanics,” SAE Technical Paper Number 851734.

20. Padmanaban, J., Moffatt, E.A., Marth, D.R., “Factors Influencing the Likelihood of Fatality and Serious/Fatal Injury in Single-Vehicle Rollover Crashes,” SAE Technical Paper Number 2005-01-0944.

21. Rains, Glen C., “Determination of the Significance of Roof Crush on Head and Neck Injury to Passenger Vehicle Occupants in Rollover Crashes,” SAE Technical Paper Number 950655.

22. Roberts, Verne L., “The Relationship between Delta-V and Injury,” SAE Technical Paper Number 933111.

23. Rose, Nathan A., “Restitution Modeling for Crush Analysis: Theory and Validation,” SAE Technical Paper Number 2006-01-0908.

24. Rose, Nathan A., “Quantifying the Uncertainty in the Coefficient of Restitution Obtained with Accelerometer Data from a Crash Test,” SAE Technical Paper Number 2007-01-0730.

25. Rose, Nathan A., Beauchamp, Gray, Fenton, Stephen J., “Factors Influencing Roof-to-Ground Impact Severity: Video Analysis and Analytical Modeling,” SAE Technical Paper Number 2007-01-0726.

26. Rose, Nathan A., Beauchamp, Gray, Fenton, Stephen J., “Analysis of Vehicle-to-Ground Impacts During a Rollover with an Impulse-Momentum Impact Model,” SAE Technical Paper Number 2008-01-0178.

27. Rose, Nathan A., et al., “A Method to Quantify Vehicle Dynamics and Deformation for Vehicle Rollover Tests Using Camera-Matching Video Analysis,” SAE Technical Paper Number 2008-01-0350.

28. Yamaguchi, Gary T., “Theoretical Analysis of a Method of Computing Dynamic Roof Crush During Rollovers,” SAE Technical Paper Number 2007-01-0366.

CONTACT INFORMATION

Nathan Rose
Kineticorp, LLC
44 Cook St., Suite 510
Denver, CO 80206
(303) 733-1888
www.kineticorp.com

APPENDIX A

This appendix presents the derivations of Equations (1) through (3) which yield the translational and rotational velocity changes for the idealized vehicle-to-ground impact shown in Figure A1.

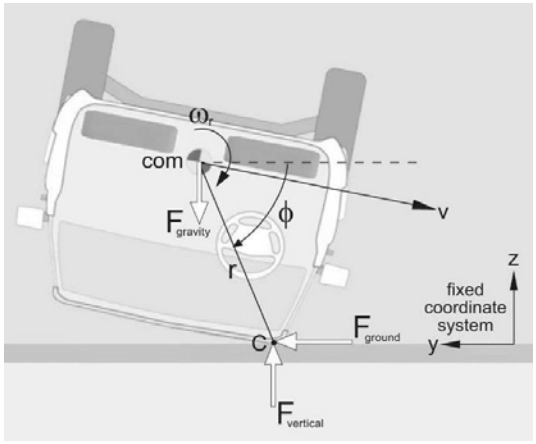

Figure A1

The development of these equations largely follows the development of the planar impact equations presented in References 3 and 4, with the exception that a gravity impulse is included.

The principle of impulse and momentum dictates the following equalities:

$$mv_{zf} - mv_{zi} = P_z - P_g \quad \text{(A1)}$$

$$mv_{yf} - mv_{yi} = P_y \quad \text{(A2)}$$

$$mk_r^2\left(\omega_{r,f} - \omega_{r,i}\right) = P_y \cdot r \cdot s\phi - P_z \cdot r \cdot c\phi \quad \text{(A3)}$$

In Equations (A1) through (A3), m is the vehicle mass, k_r is the vehicle's radius of gyration for the roll axis, r is the distance between the vehicle's CoM and the point at which the impact force is applied (Point C), ϕ is the angle between the orientation of the ground plane and the line connecting the CoM to Point C, P_z and P_y are the normal (vertical) and tangential (ground plane) impulse components that result from the impact and P_g is the gravity impulse. Translational velocity components are denoted with the letter v and final and initial velocities are denoted with the subscripts *f* and *i*.

The following constraint equations govern the impact energy loss along the normal and tangential directions:

$$e = -\frac{v_{zf} - r \cdot c\phi \cdot \omega_{r,f}}{v_{zi} - r \cdot c\phi \cdot \omega_{r,i}} \quad \text{(A4)}$$

$$\mu = \frac{P_y}{P_z} \quad \text{(A5)}$$

In Equations (A4), e is the coefficient of restitution for the impact, which is defined as the negative ratio of the post-impact to pre-impact vertical velocities at the point of collision force transfer (Point C). In Equation (A5), μ is the impulse ratio, which establishes the magnitude of the tangential impulse relative to the magnitude of the normal impulse. This equation yields Equation (2) in the main body of this paper when Equations (A1) and (A2) are substituted into it.

Substituting Equation (A5) into (A3) yields the following equation:

$$m \cdot k_r^2 \cdot \left(\omega_{r,f} - \omega_{r,i}\right) = P_z \cdot r \cdot \left(\mu \cdot s\phi - c\phi\right) \quad \text{(A6)}$$

Then, the following equation results from substituting Equation (A1) into (A6):

$$m \cdot k_r^2 \cdot \Delta\omega_r = \left(m\Delta V_z + P_g\right) \cdot r \cdot \left(\mu \cdot s\phi - c\phi\right) \quad \text{(A7)}$$

The gravity impulse can be rewritten with the following equation, which can then be substituted into Equation (A7) to yield Equation (A9):

$$P_g = mg \cdot \Delta t_i \quad \text{(A8)}$$

$$m \cdot k_r^2 \cdot \Delta\omega_r = \left(m\Delta V_z + mg\Delta t_i\right) \cdot r \cdot \left(\mu \cdot s\phi - c\phi\right) \quad \text{(A9)}$$

In Equation (A8), g is the gravitational constant and Δt_i is the impact duration. Algebraic manipulation of Equation (A9) yields Equation (A10), which is equivalent to Equation (3) in the main body of this paper.

$$\Delta\omega_r = \omega_{r,f} - \omega_{r,i} = \left(\Delta V_z + g \cdot \Delta t_i\right) \cdot \frac{r \cdot \left(\mu \cdot s\phi - c\phi\right)}{k_r^2} \quad \text{(A10)}$$

Now, algebraically manipulate Equation (A4) to solve for the final roll velocity:

$$\omega_{r,f} = \frac{1}{r \cdot c\phi} v_{zf} + \frac{e}{r \cdot c\phi}\left(v_{zi} - r \cdot c\phi \cdot \omega_{r,i}\right) \quad \text{(A11)}$$

Now, equate Equations (A10) and (A11) through the final roll velocity and algebraically manipulate to obtain the following equation:

$$\Delta V_z = -(1+e) \cdot v_{zc,i} \cdot \left\{\frac{k_r^2}{k_r^2 + r^2\left(c^2\phi - \mu \cdot s\phi \cdot c\phi\right)}\right\} - g \cdot \Delta t_i \cdot \left\{\frac{r^2\left(c^2\phi - \mu \cdot s\phi \cdot c\phi\right)}{k_r^2 + r^2\left(c^2\phi - \mu \cdot s\phi \cdot c\phi\right)}\right\} \quad \text{(A12)}$$

Equation (A12) is equivalent to Equation (1) in the main body of this paper.

The Effect of Impact Angle and Roll Velocity on the Upward CoM Velocity Change
(SUV, Translational Speed = 40 mph, Downward Speed = 2 mph, e=0, r=3.0 ft, Δt = 300ms)

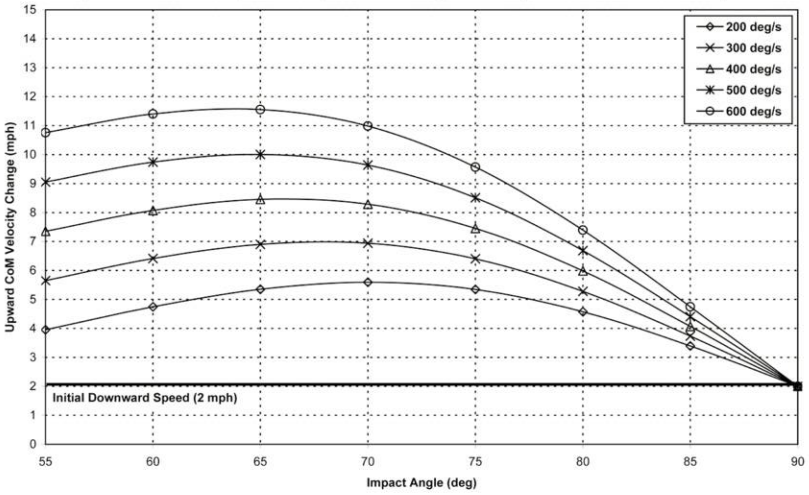

The Effect of Impact Angle and Roll Velocity on the Upward CoM Velocity Change
(SUV, Translational Speed = 30 mph, Downward Speed = 2 mph, e=0, r=3.0 ft, Δt = 300ms)

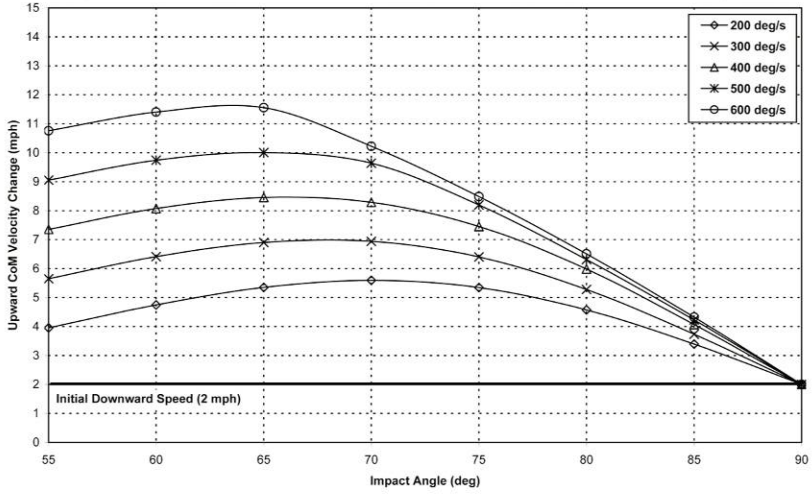

The Effect of Impact Angle and Roll Velocity on the Upward CoM Velocity Change
(SUV, Translational Speed = 20 mph, Downward Speed = 2 mph, e=0, r=3.0 ft, Δt = 300ms)

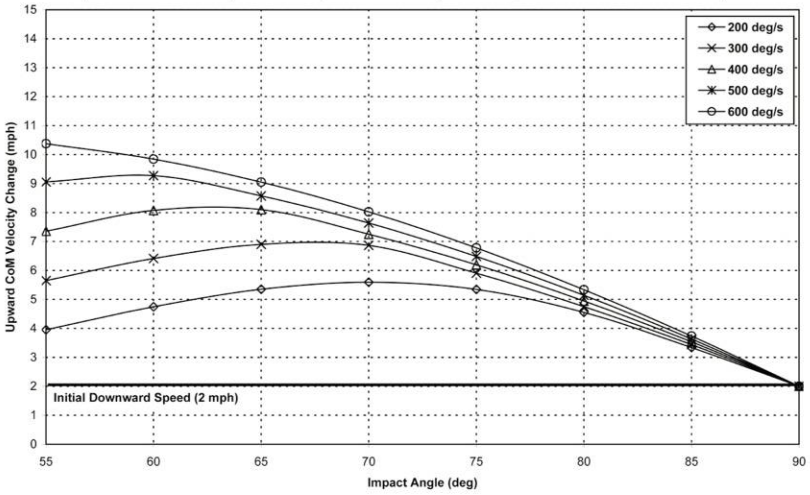

The Effect of Impact Angle and Roll Velocity on the Updward CoM Velocity Change
(SUV, Translational Speed = 10 mph, Downward Speed = 2 mph, e=0, r=3.0 ft, Δt = 300ms)

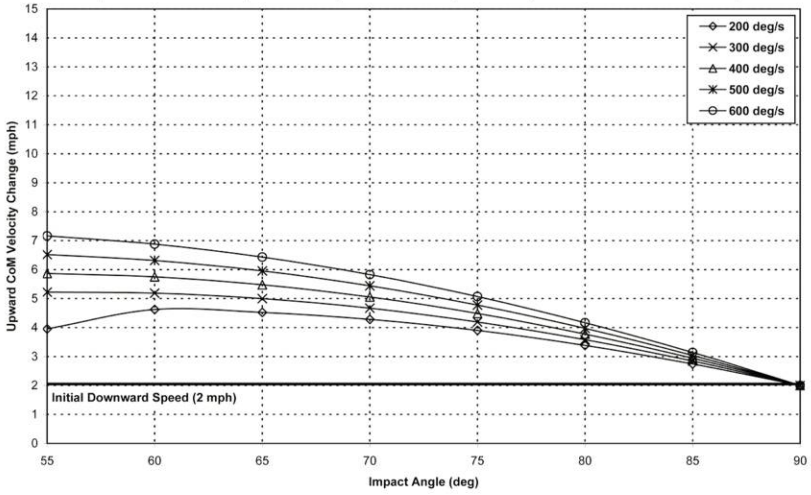

A1 - Vehicle-to-Ground Impact Scenarios (ΔV_z)

The Effect of Impact Angle and Roll Velocity on the Upward CoM Velocity Change
(SUV, Translational Speed = 40 mph, Downward Speed = 2 mph, e=0, r=2.5 ft, Δt = 300ms)

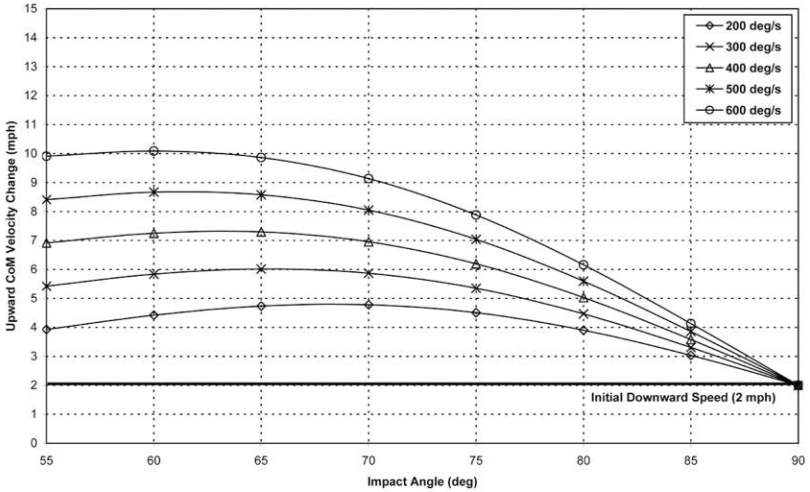

The Effect of Impact Angle and Roll Velocity on the Upward CoM Velocity Change
(SUV, Translational Speed = 30 mph, Downward Speed = 2 mph, e=0, r=2.5 ft, Δt = 300ms)

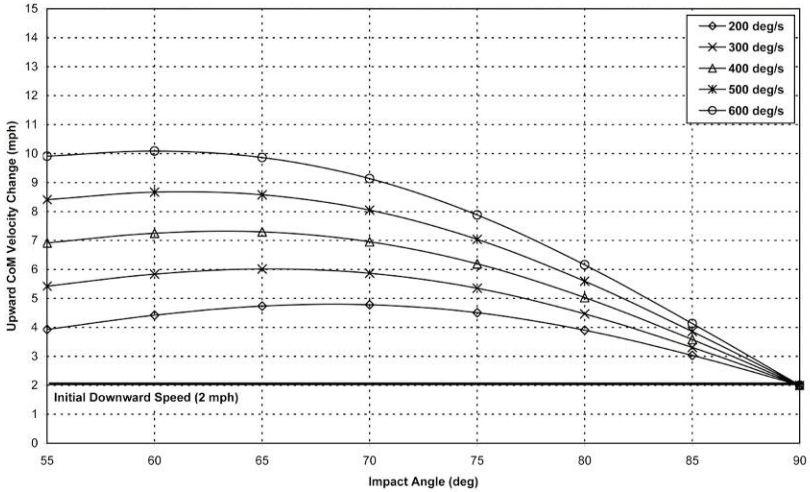

The Effect of Impact Angle and Roll Velocity on the Upward CoM Velocity Change
(SUV, Translational Speed = 20 mph, Downward Speed = 2 mph, e=0, r=2.5 ft, Δt = 300ms)

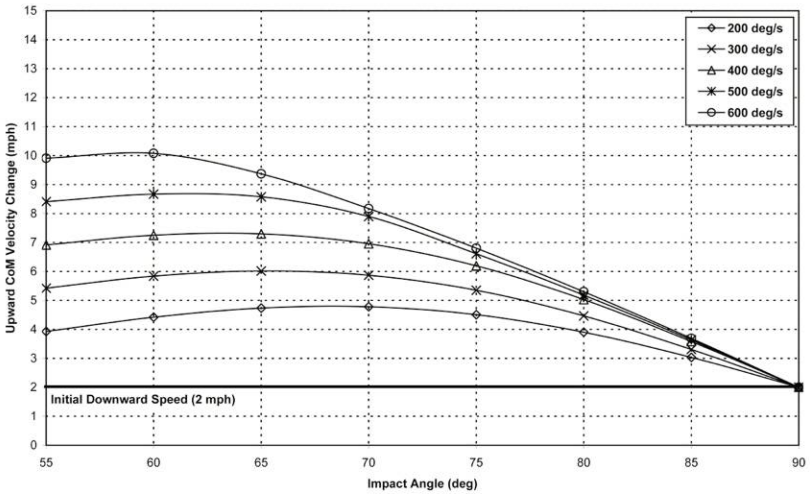

The Effect of Impact Angle and Roll Velocity on the Updward CoM Velocity Change
(SUV, Translational Speed = 10 mph, Downward Speed = 2 mph, e=0, r=2.5 ft, Δt = 300ms)

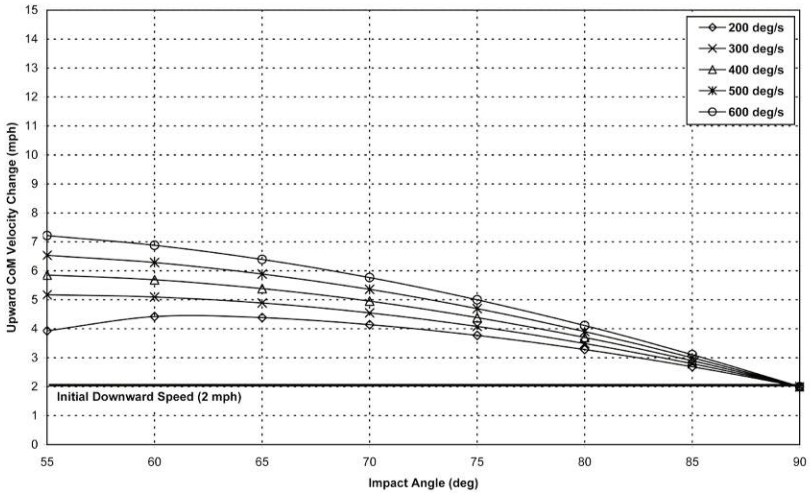

A2 - Vehicle-to-Ground Impact Scenarios (ΔV_z)

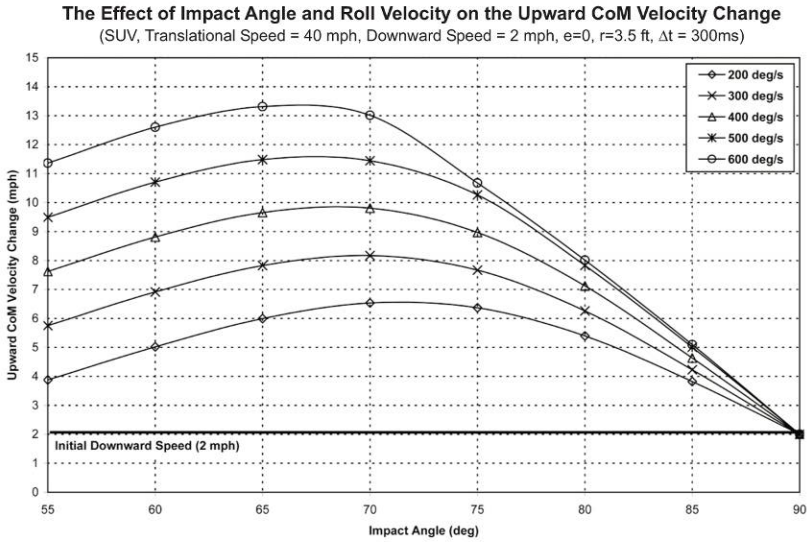

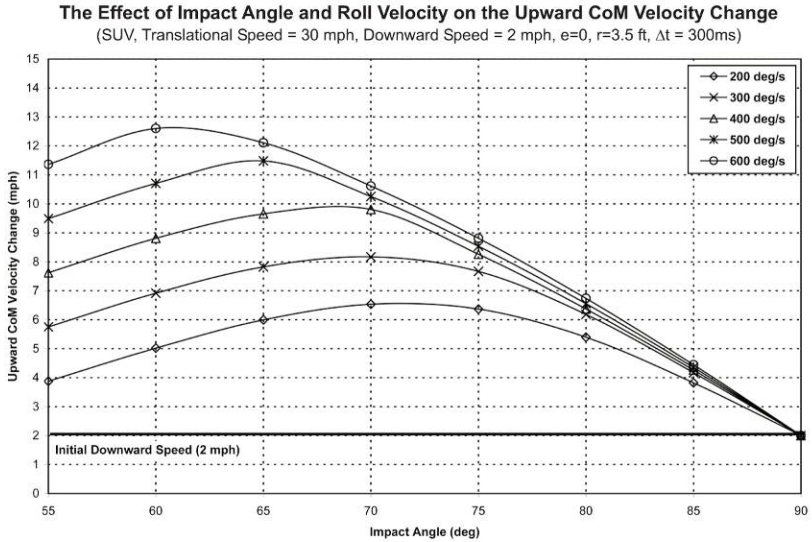

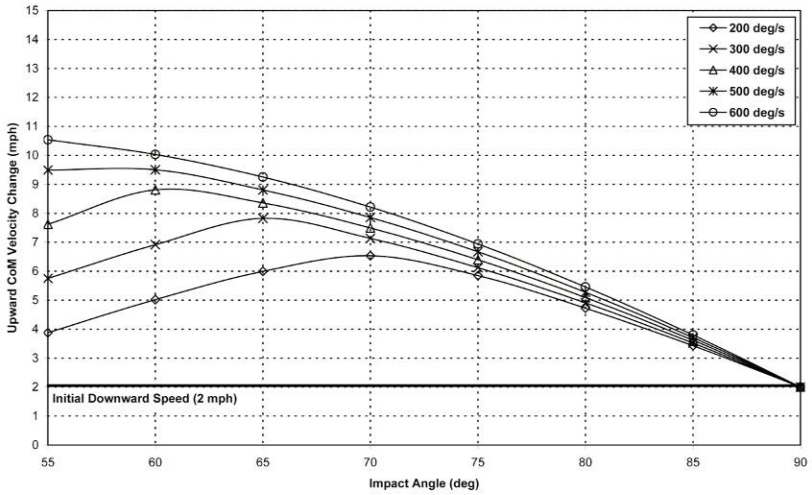

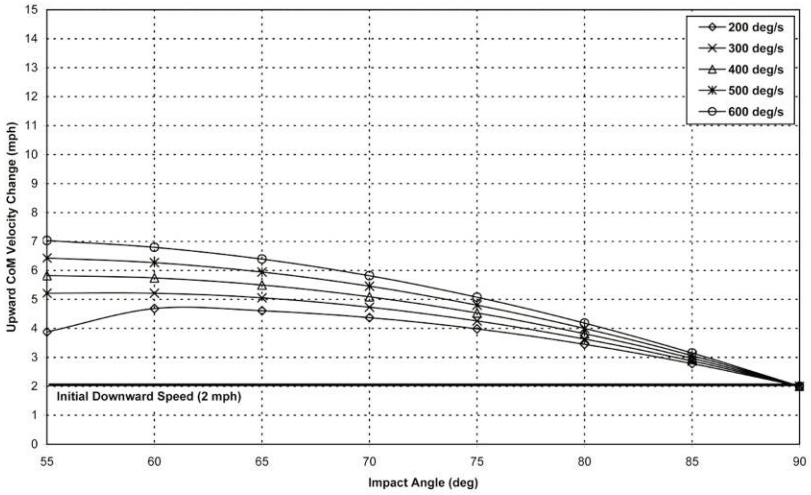

A3 - Vehicle-to-Ground Impact Scenarios (ΔV_z)

The Effect of Impact Angle and Roll Velocity on the Upward CoM Velocity Change
(SUV, Translational Speed = 40 mph, Downward Speed = 4 mph, e=0, r=3.0 ft, Δt = 300ms)

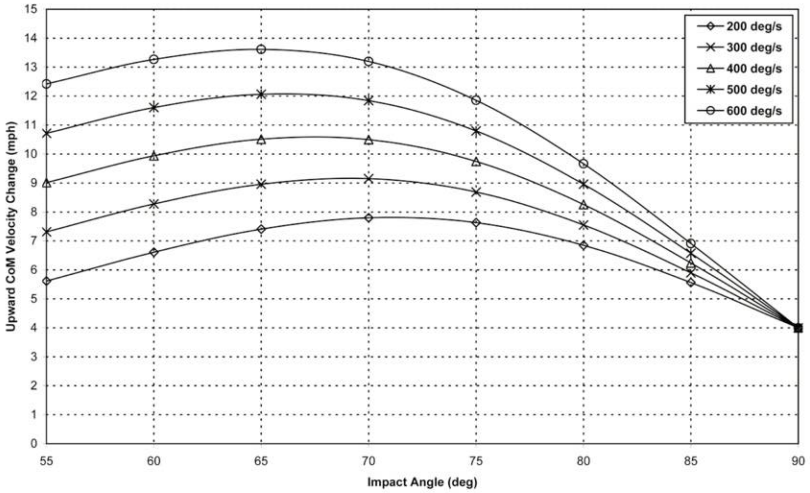

The Effect of Impact Angle and Roll Velocity on the Upward CoM Velocity Change
(SUV, Translational Speed = 30 mph, Downward Speed = 4 mph, e=0, r=3.0 ft, Δt = 300ms)

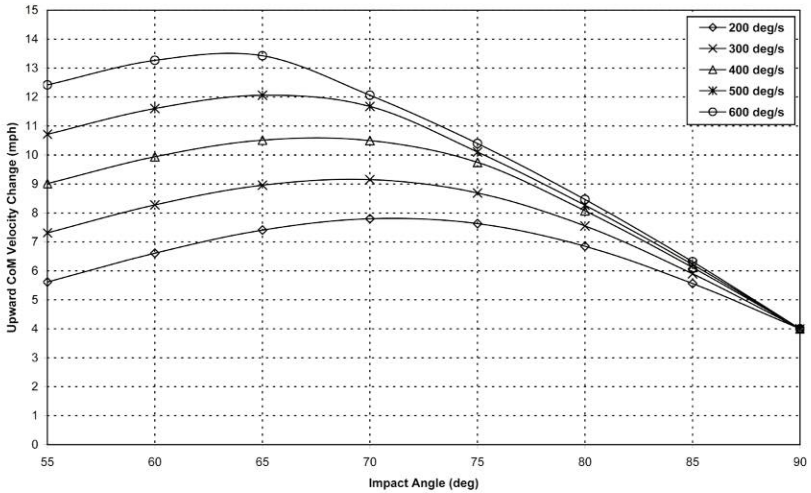

The Effect of Impact Angle and Roll Velocity on the Upward CoM Velocity Change
(SUV, Translational Speed = 20 mph, Downward Speed = 4 mph, e=0, r=3.0 ft, Δt = 300ms)

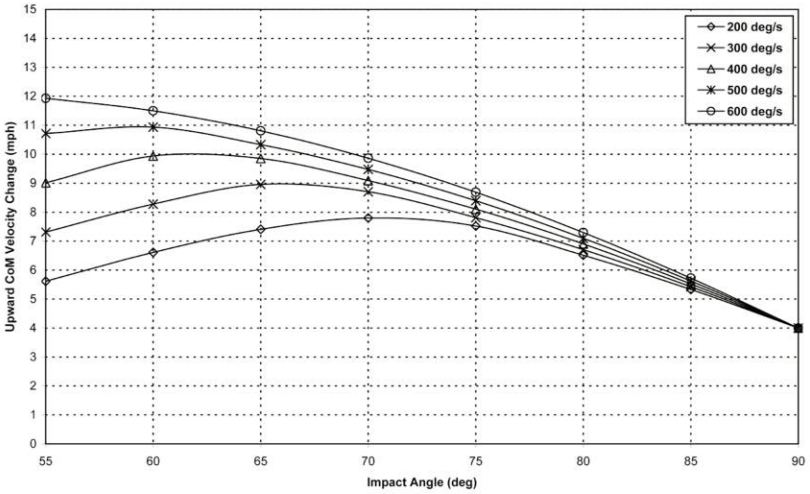

The Effect of Impact Angle and Roll Velocity on the Updward CoM Velocity Change
(SUV, Translational Speed = 10 mph, Downward Speed = 4 mph, e=0, r=3.0 ft, Δt = 300ms)

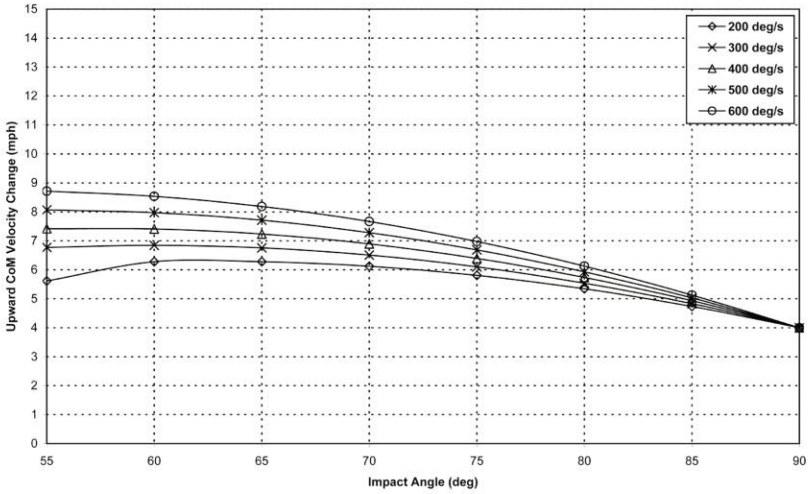

A4 - Vehicle-to-Ground Impact Scenarios (ΔV_z)

The Effect of Impact Angle and Roll Velocity on the Upward CoM Velocity Change
(SUV (k=1.8 ft), Translational Speed = 40 mph, Downward Speed = 2 mph, e=0, r=3.0 ft, Δt = 300ms)

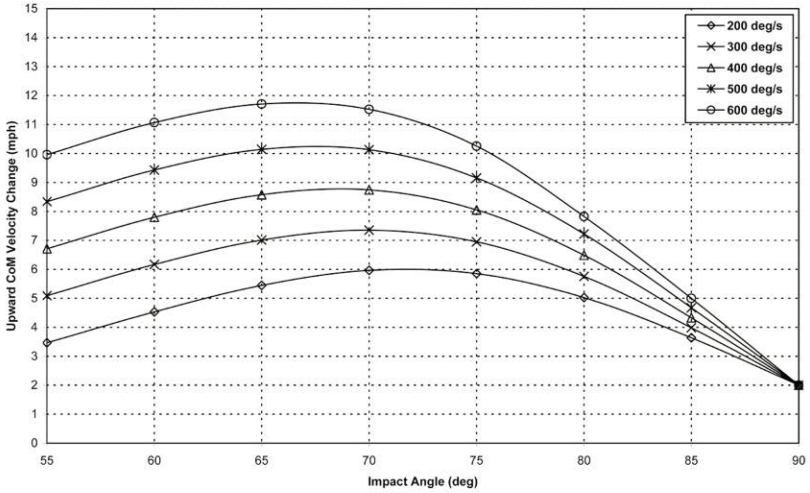

The Effect of Impact Angle and Roll Velocity on the Upward CoM Velocity Change
(SUV (k=1.8 ft), Translational Speed = 30 mph, Downward Speed = 2 mph, e=0, r=3.0 ft, Δt = 300ms)

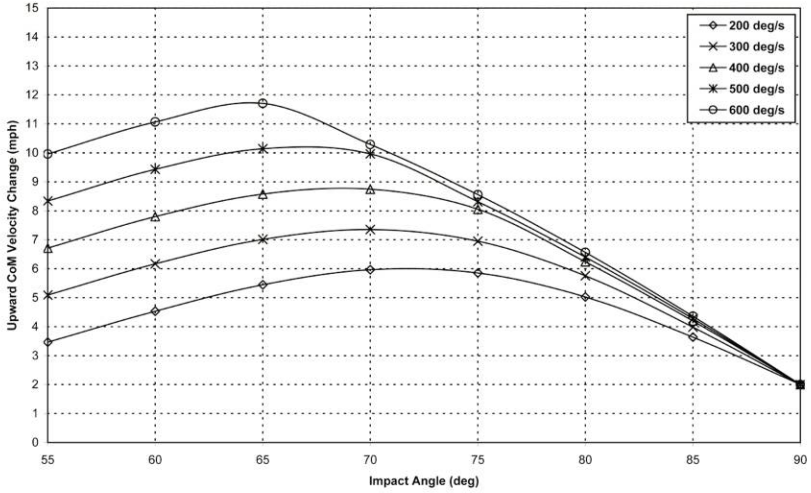

The Effect of Impact Angle and Roll Velocity on the Upward CoM Velocity Change
(SUV (k = 1.8 ft), Translational Speed = 20 mph, Downward Speed = 2 mph, e=0, r=3.0 ft, Δt = 300ms)

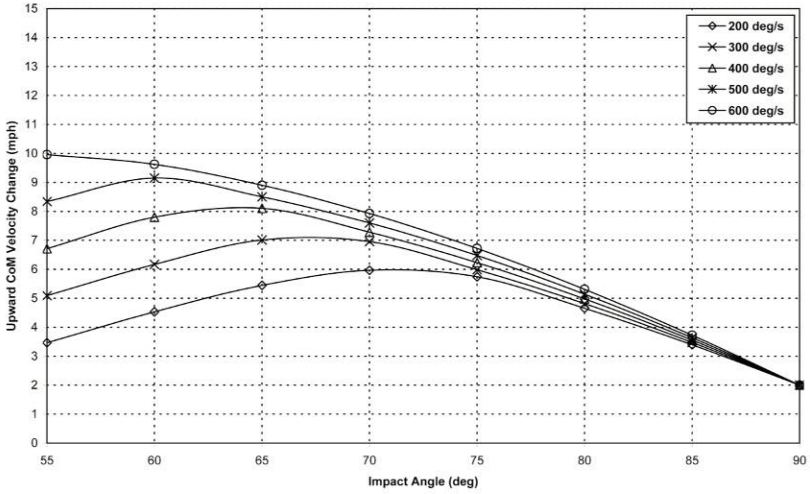

The Effect of Impact Angle and Roll Velocity on the Updward CoM Velocity Change
(SUV (k=1.8 ft), Translational Speed = 10 mph, Downward Speed = 2 mph, e=0, r=3.0 ft, Δt = 300ms)

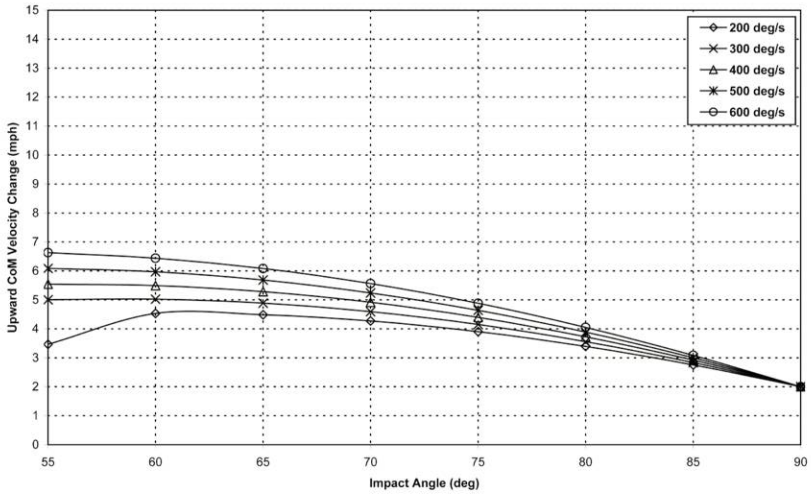

A5 - Vehicle-to-Ground Impact Scenarios (ΔV_z)

The Effect of Impact Angle and Roll Velocity on the Upward CoM Velocity Change
(SUV (k=2.3 ft), Translational Speed = 40 mph, Downward Speed = 2 mph, e=0, r=3.0 ft, Δt = 300ms)

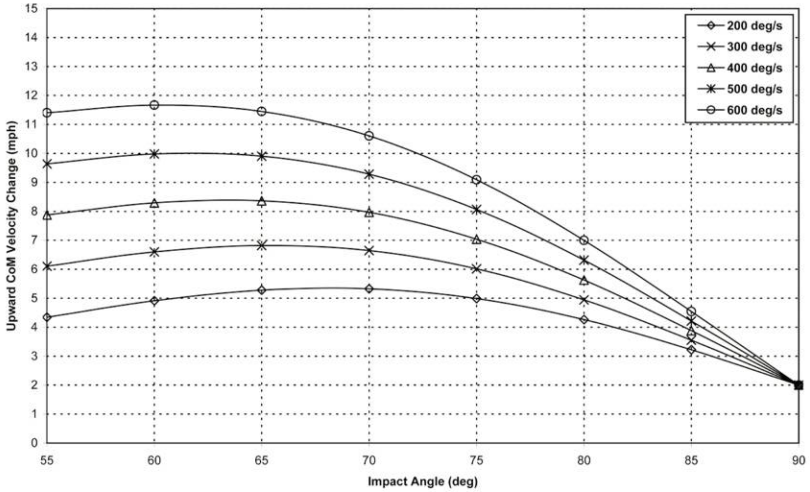

The Effect of Impact Angle and Roll Velocity on the Upward CoM Velocity Change
(SUV (k=2.3 ft), Translational Speed = 30 mph, Downward Speed = 2 mph, e=0, r=3.0 ft, Δt = 300ms)

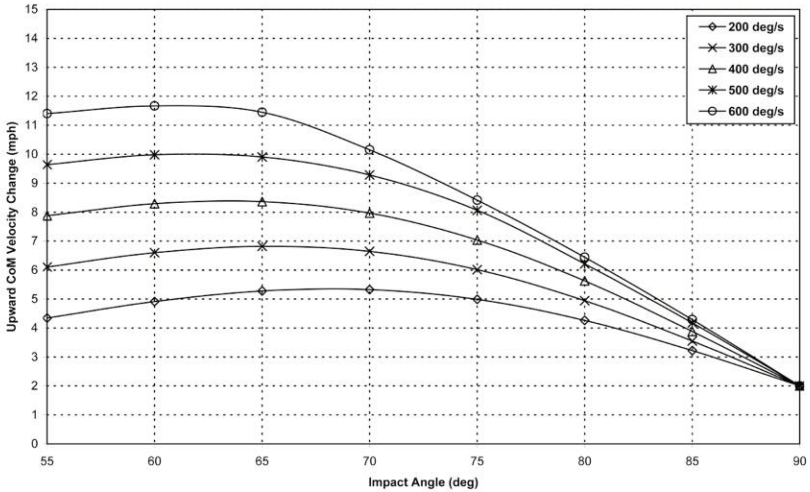

The Effect of Impact Angle and Roll Velocity on the Upward CoM Velocity Change
(SUV (k = 2.3 ft), Translational Speed = 20 mph, Downward Speed = 2 mph, e=0, r=3.0 ft, Δt = 300ms)

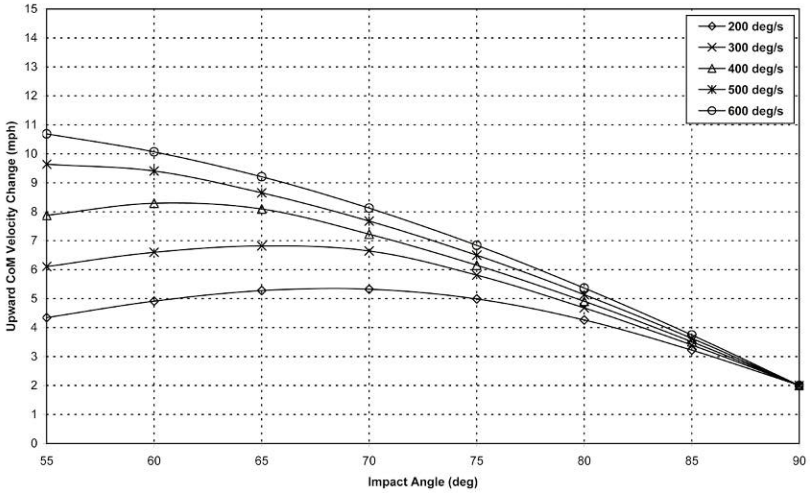

The Effect of Impact Angle and Roll Velocity on the Updward CoM Velocity Change
(SUV (k=2.3 ft), Translational Speed = 10 mph, Downward Speed = 2 mph, e=0, r=3.0 ft, Δt = 300ms)

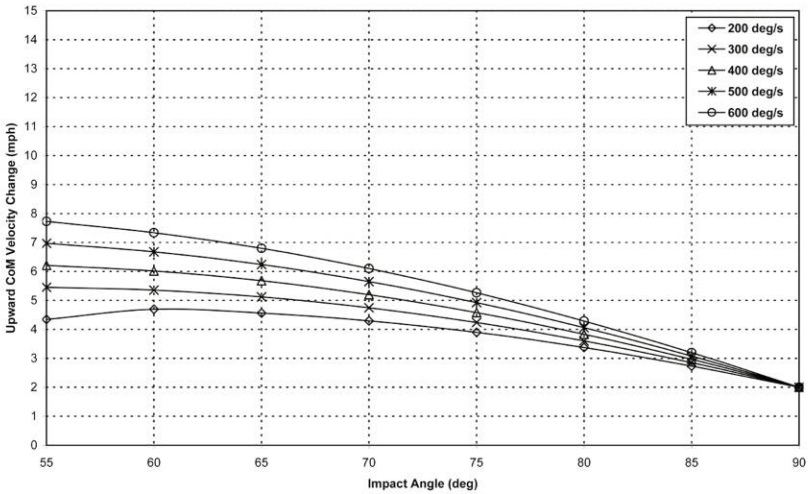

A6 - Vehicle-to-Ground Impact Scenarios (ΔV_z)

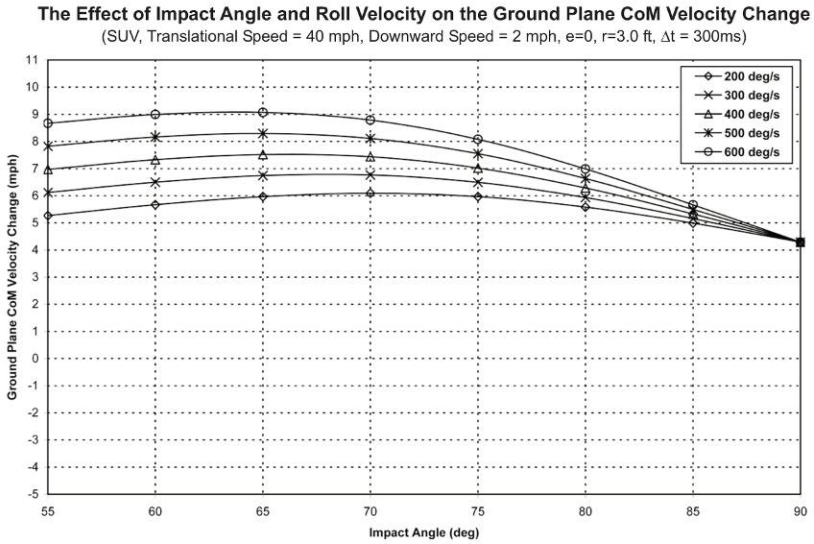

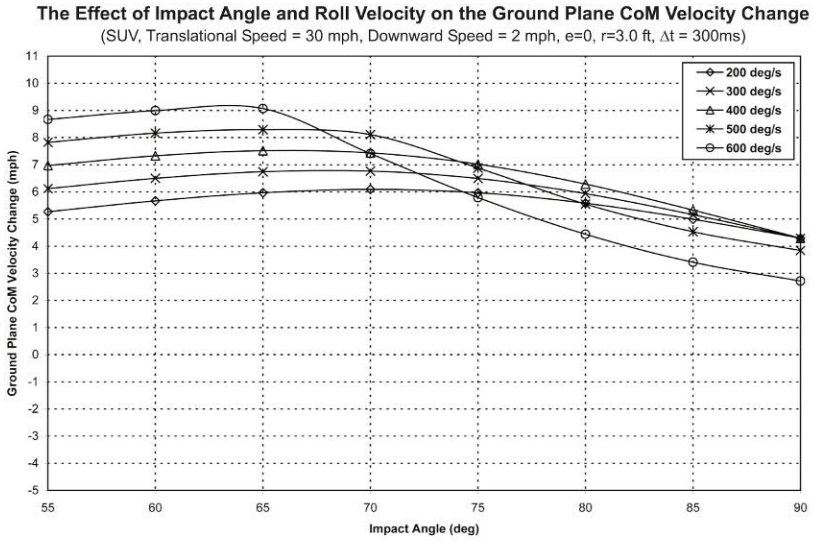

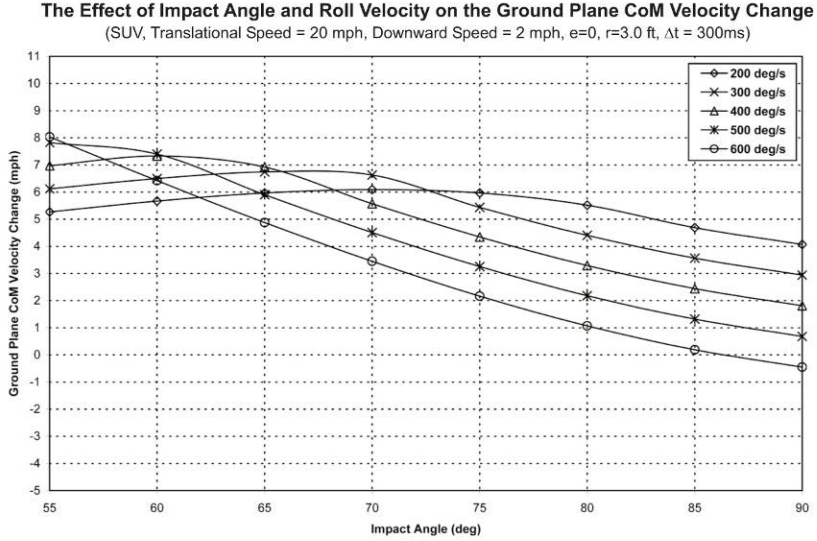

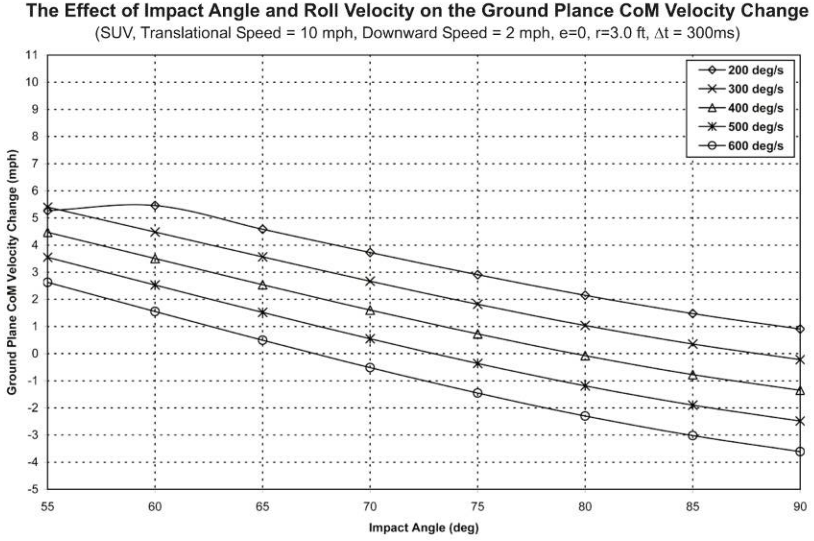

B1 - Vehicle-to-Ground Impact Scenarios (ΔV_y)

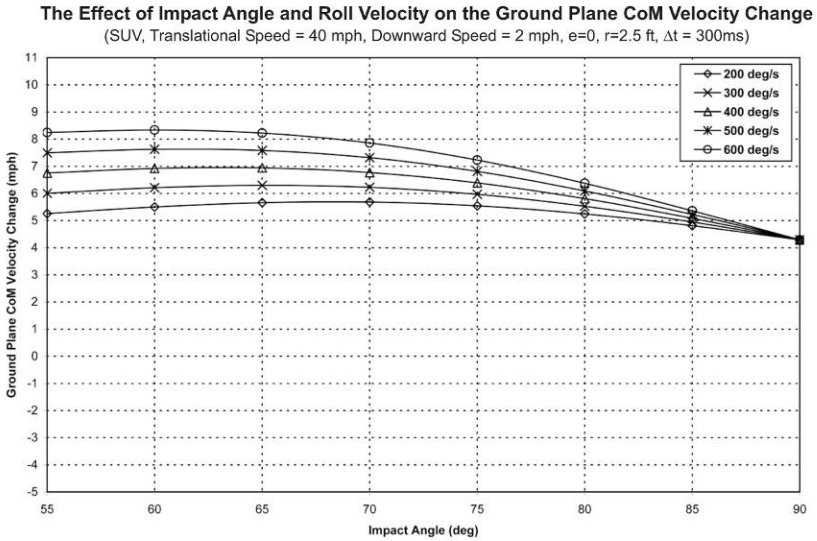
The Effect of Impact Angle and Roll Velocity on the Ground Plane CoM Velocity Change
(SUV, Translational Speed = 40 mph, Downward Speed = 2 mph, e=0, r=2.5 ft, Δt = 300ms)
Ground Plane CoM Velocity Change (mph)
Impact Angle (deg)
200 deg/s
300 deg/s
400 deg/s
500 deg/s
600 deg/s

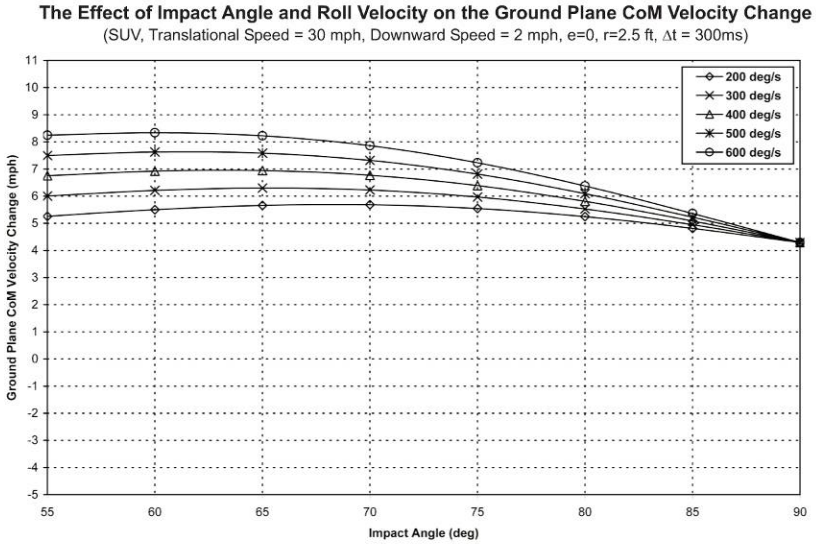
The Effect of Impact Angle and Roll Velocity on the Ground Plane CoM Velocity Change
(SUV, Translational Speed = 30 mph, Downward Speed = 2 mph, e=0, r=2.5 ft, Δt = 300ms)
Ground Plane CoM Velocity Change (mph)
Impact Angle (deg)
200 deg/s
300 deg/s
400 deg/s
500 deg/s
600 deg/s

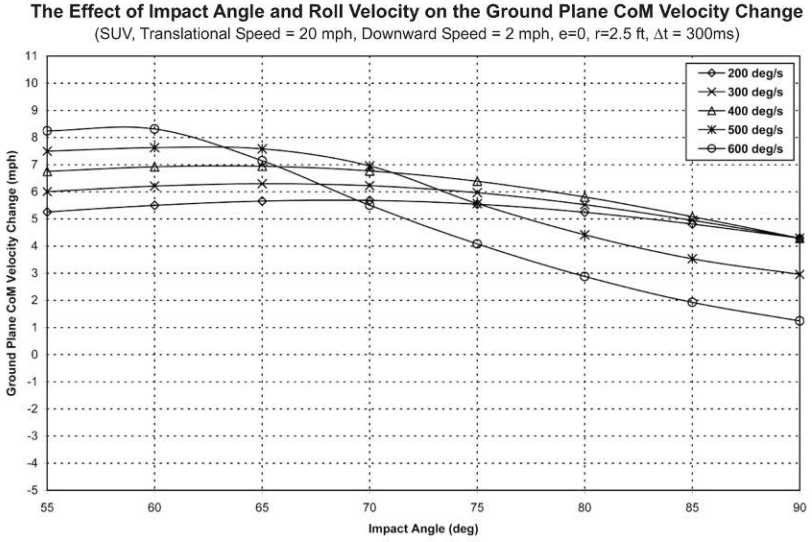
The Effect of Impact Angle and Roll Velocity on the Ground Plane CoM Velocity Change
(SUV, Translational Speed = 20 mph, Downward Speed = 2 mph, e=0, r=2.5 ft, Δt = 300ms)
Ground Plane CoM Velocity Change (mph)
Impact Angle (deg)
200 deg/s
300 deg/s
400 deg/s
500 deg/s
600 deg/s

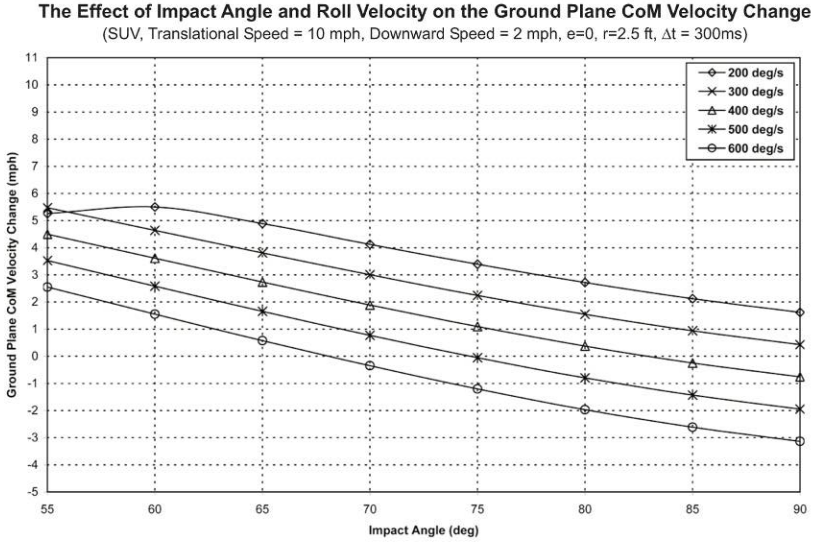
The Effect of Impact Angle and Roll Velocity on the Ground Plane CoM Velocity Change
(SUV, Translational Speed = 10 mph, Downward Speed = 2 mph, e=0, r=2.5 ft, Δt = 300ms)
Ground Plane CoM Velocity Change (mph)
Impact Angle (deg)
200 deg/s
300 deg/s
400 deg/s
500 deg/s
600 deg/s

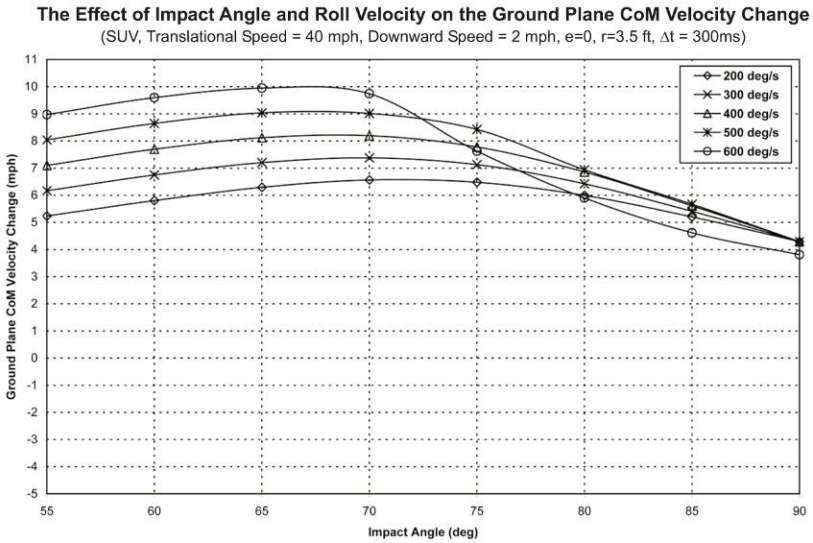

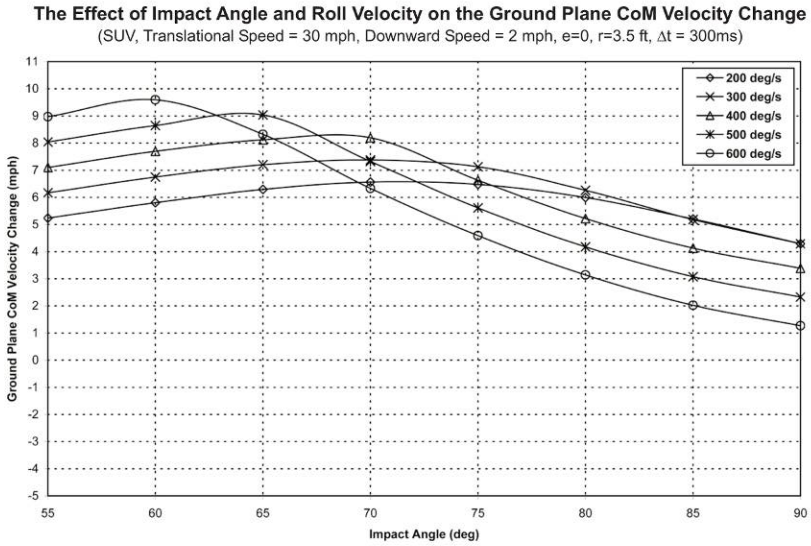

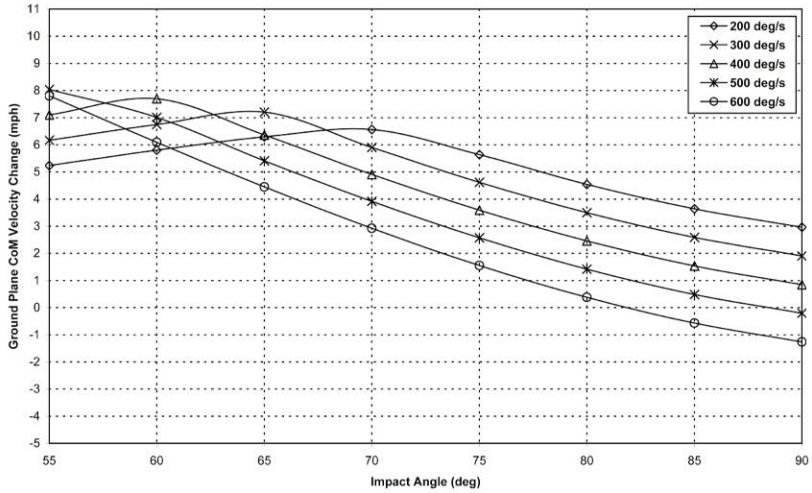

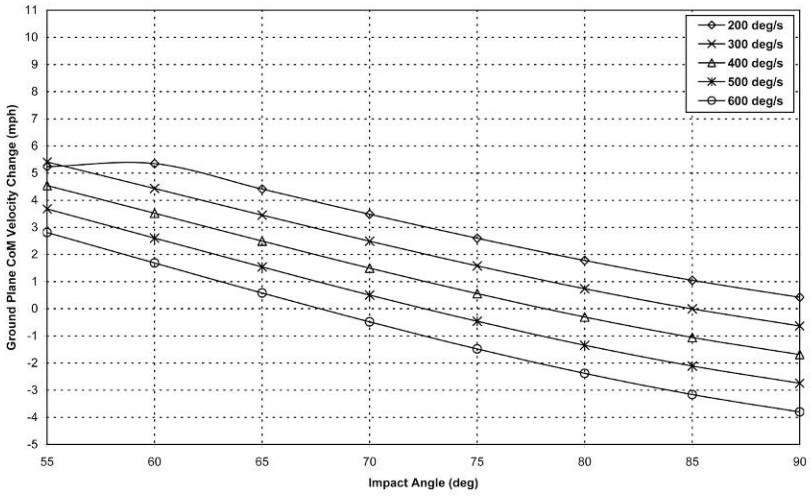

B3 - Vehicle-to-Ground Impact Scenarios (ΔV_y)

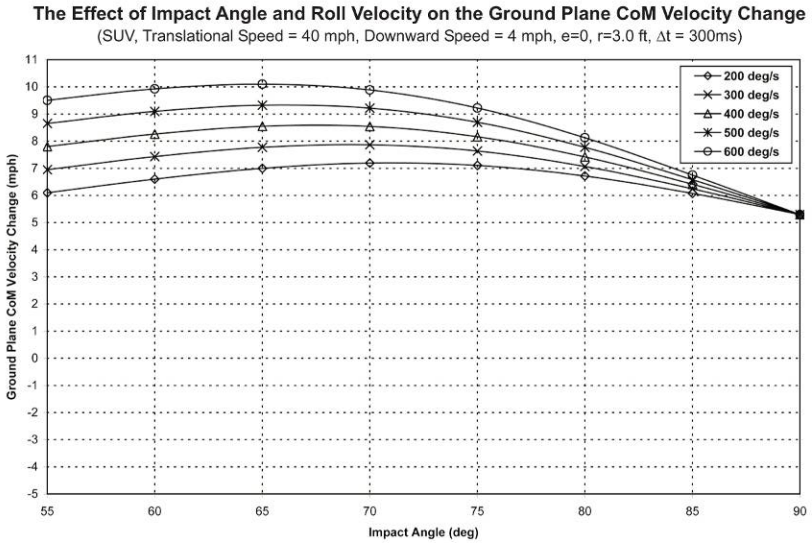

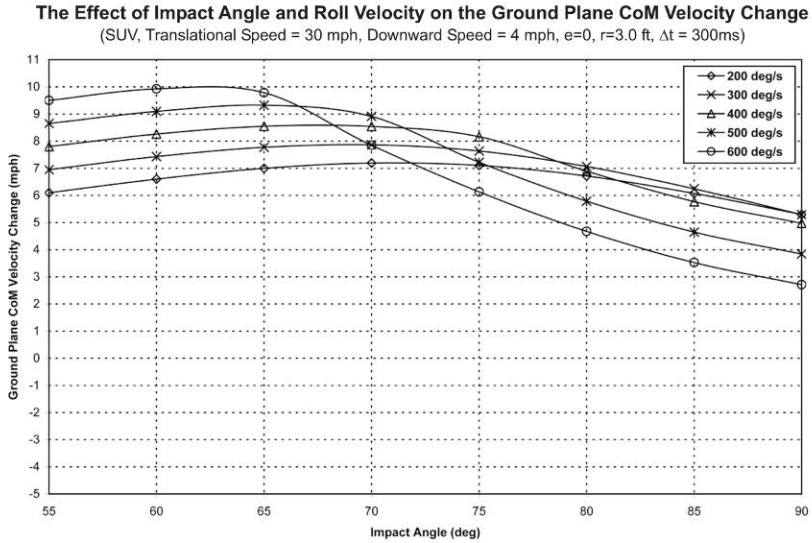

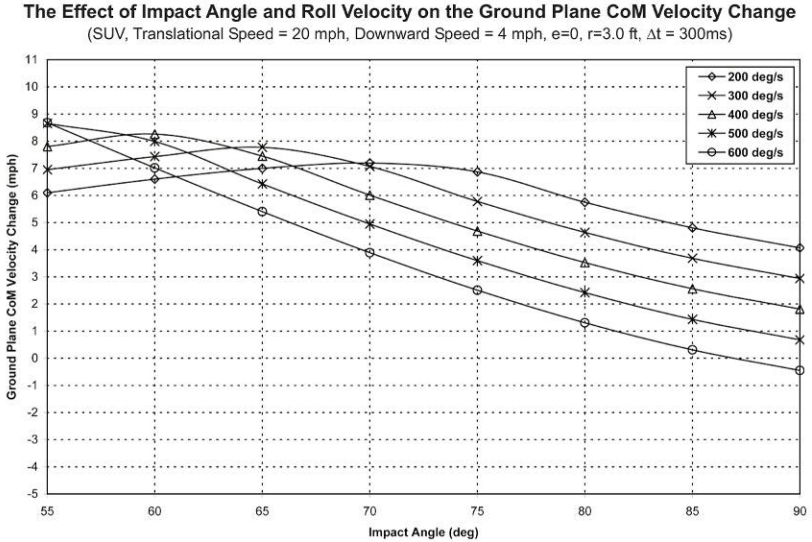

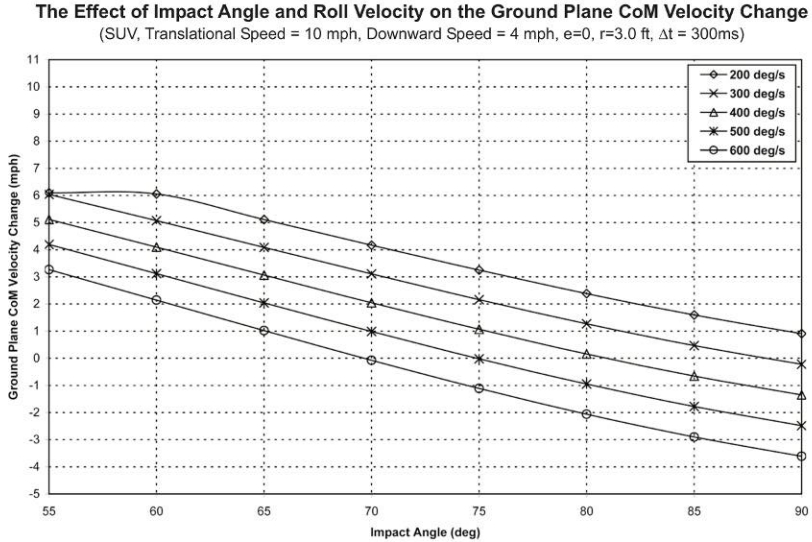

B4 - Vehicle-to-Ground Impact Scenarios (ΔV_y)

The Effect of Impact Angle and Roll Velocity on the Change in Roll Velocity
(SUV, Translational Speed = 40 mph, Downward Speed = 2 mph, e=0, r=3.0 ft, Δt = 300ms)

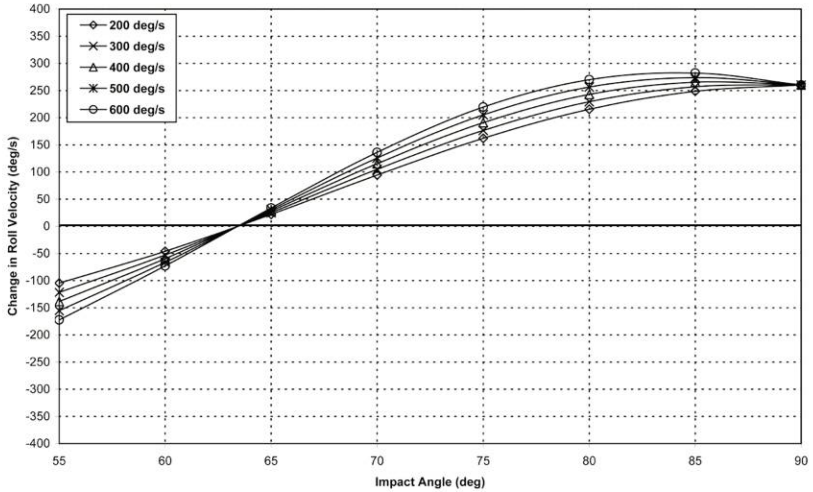

The Effect of Impact Angle and Roll Velocity on the Change in Roll Velocity
(SUV, Translational Speed = 30 mph, Downward Speed = 2 mph, e=0, r=3.0 ft, Δt = 300ms)

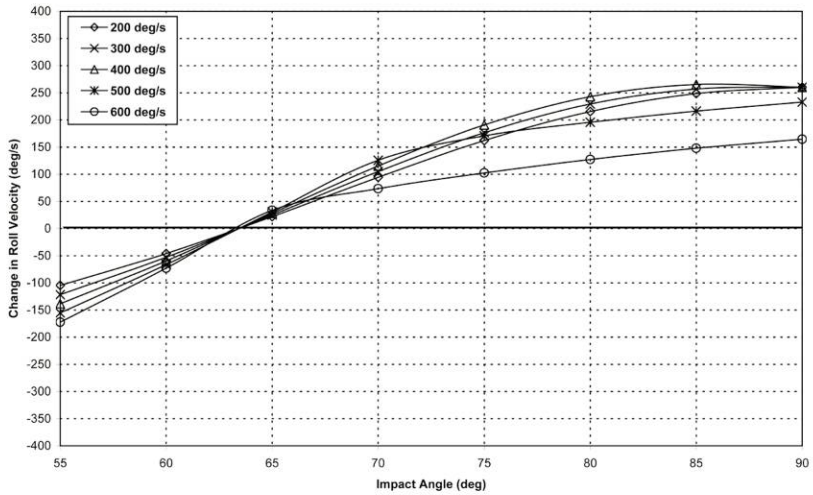

The Effect of Impact Angle and Roll Velocity on the Change in Roll Velocity
(SUV, Translational Speed = 20 mph, Downward Speed = 2 mph, e=0, r=3.0 ft, Δt = 300ms)

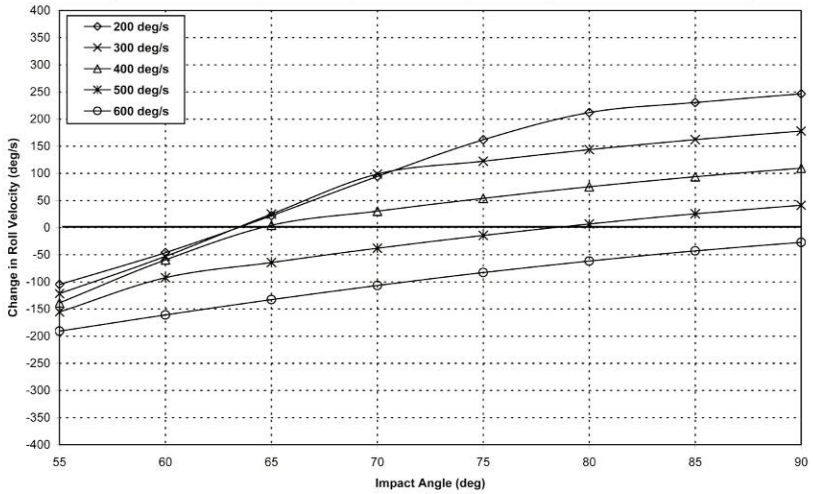

The Effect of Impact Angle and Roll Velocity on the Change in Roll Velocity
(SUV, Translational Speed = 10 mph, Downward Speed = 2 mph, e=0, r=3.0 ft, Δt = 300ms)

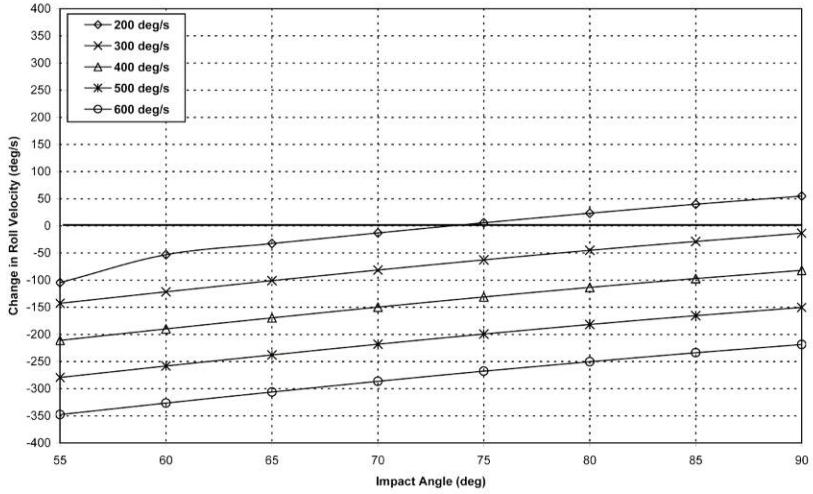

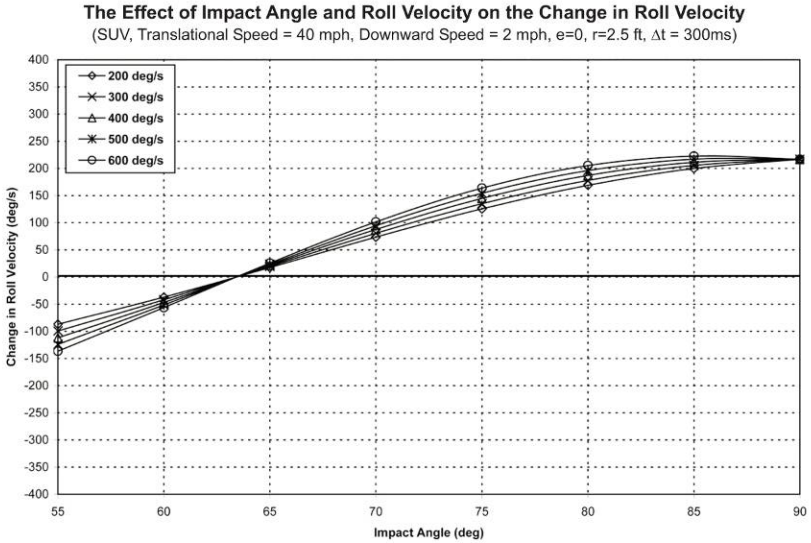

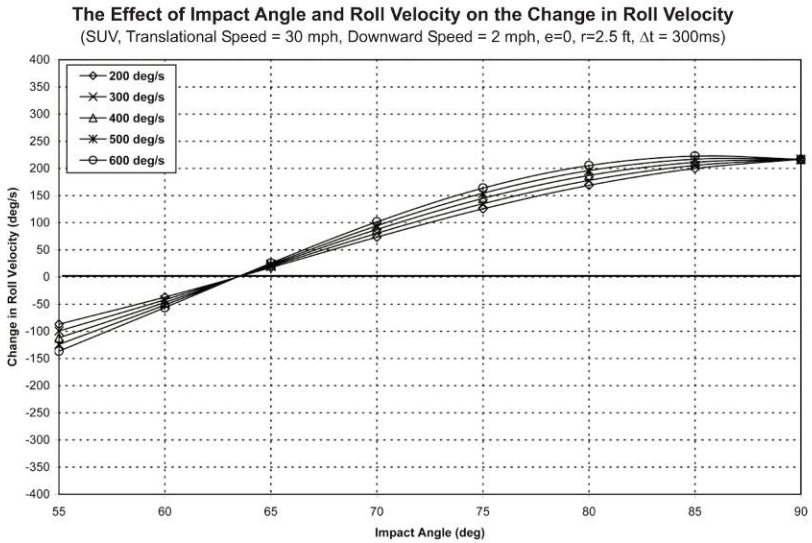

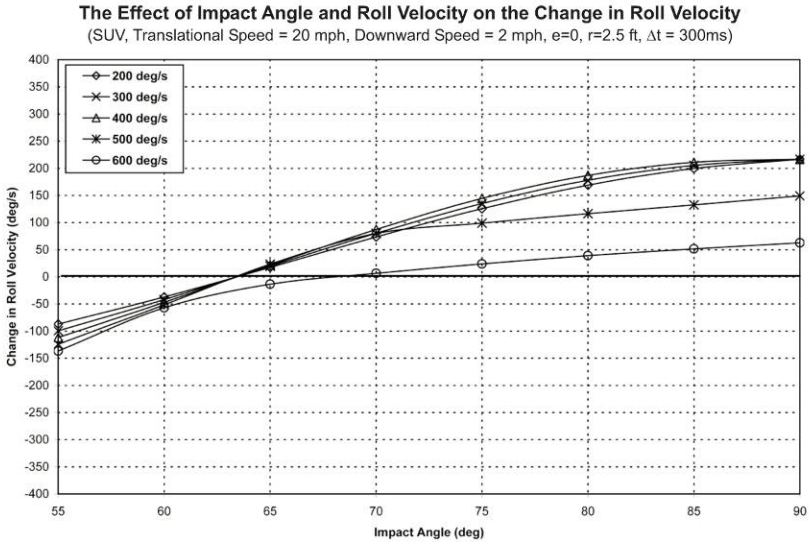

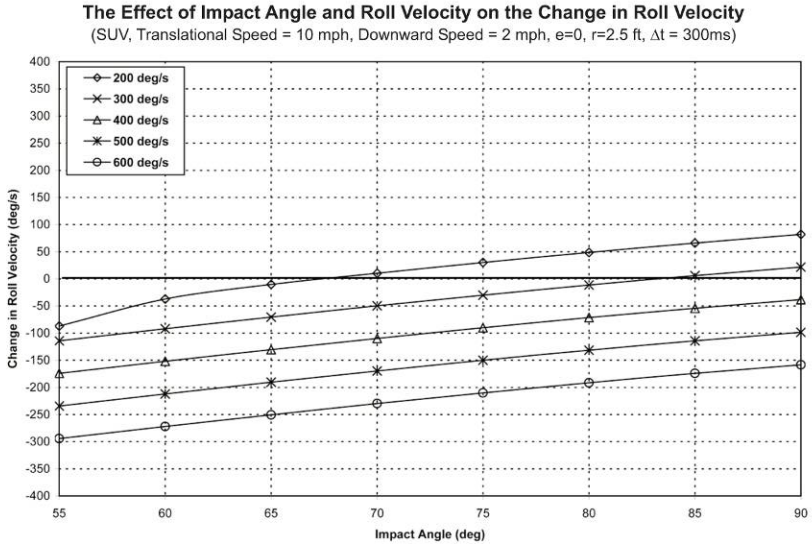

C2 - Vehicle-to-Ground Impact Scenarios ($\Delta\omega$)

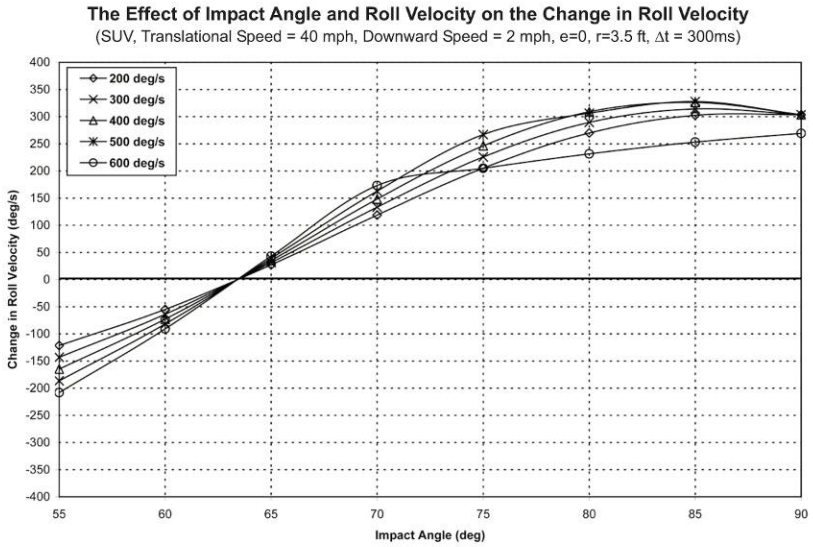

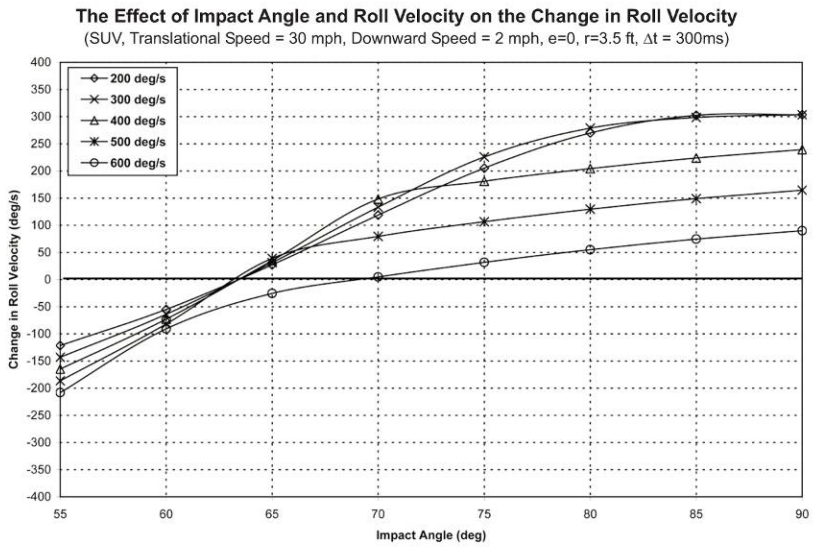

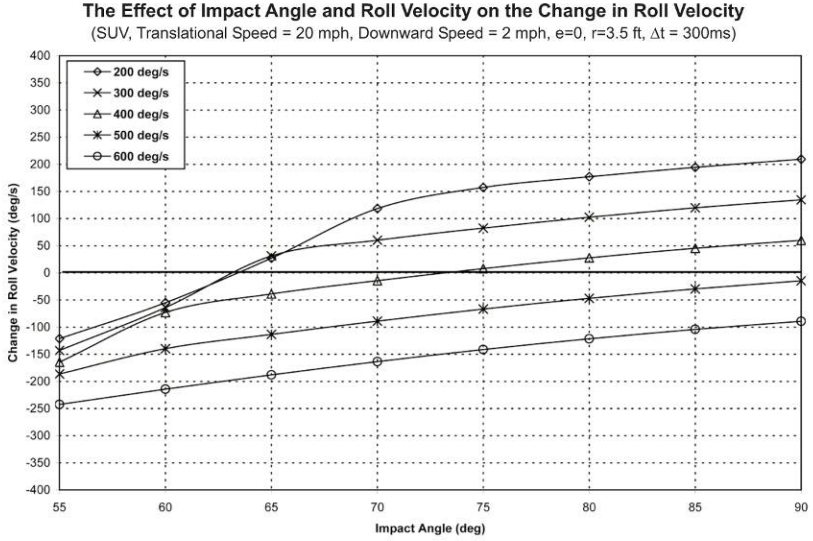

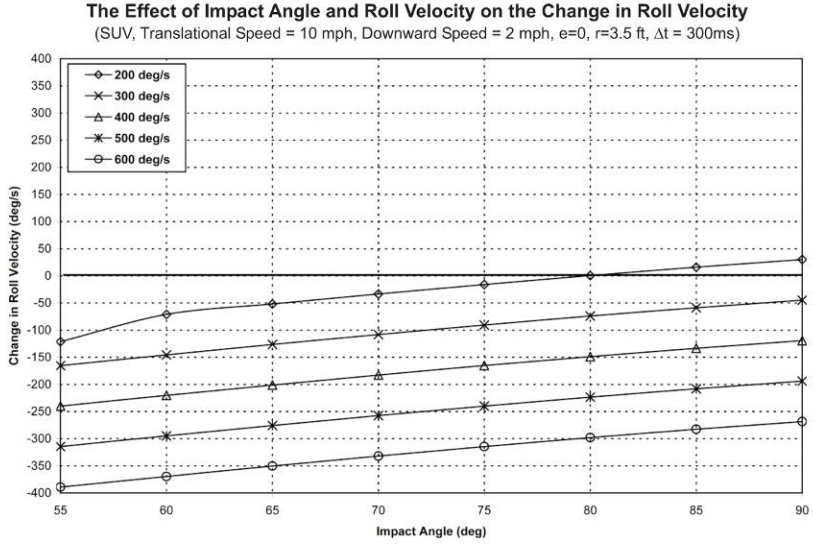

C3 - Vehicle-to-Ground Impact Scenarios ($\Delta\omega$)

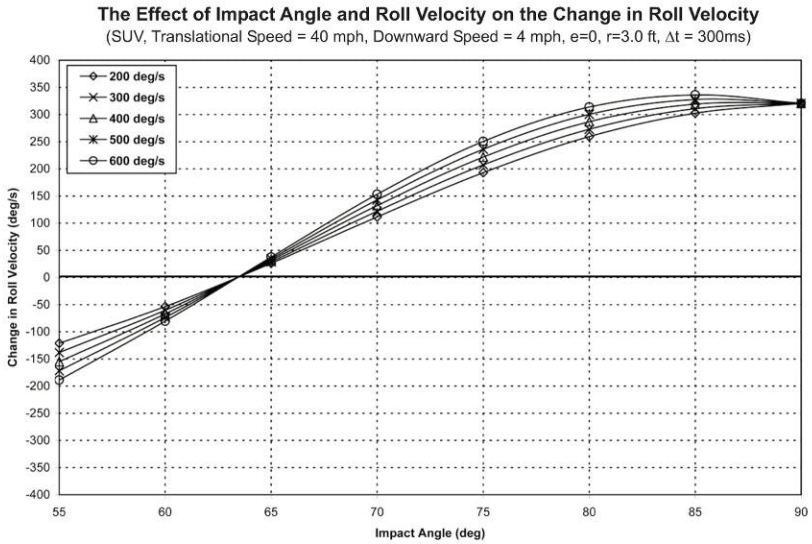
The Effect of Impact Angle and Roll Velocity on the Change in Roll Velocity
(SUV, Translational Speed = 40 mph, Downward Speed = 4 mph, e=0, r=3.0 ft, Δt = 300ms)
200 deg/s
300 deg/s
400 deg/s
500 deg/s
600 deg/s
Change in Roll Velocity (deg/s)
Impact Angle (deg)

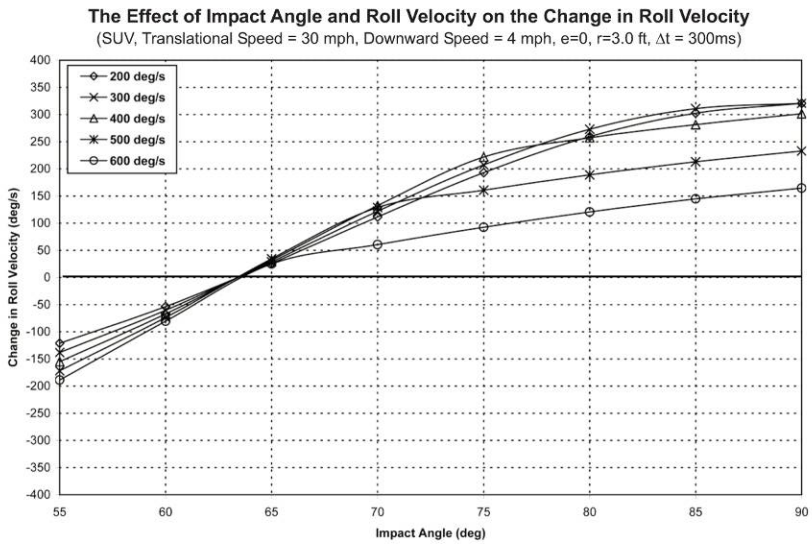
The Effect of Impact Angle and Roll Velocity on the Change in Roll Velocity
(SUV, Translational Speed = 30 mph, Downward Speed = 4 mph, e=0, r=3.0 ft, Δt = 300ms)
200 deg/s
300 deg/s
400 deg/s
500 deg/s
600 deg/s
Change in Roll Velocity (deg/s)
Impact Angle (deg)

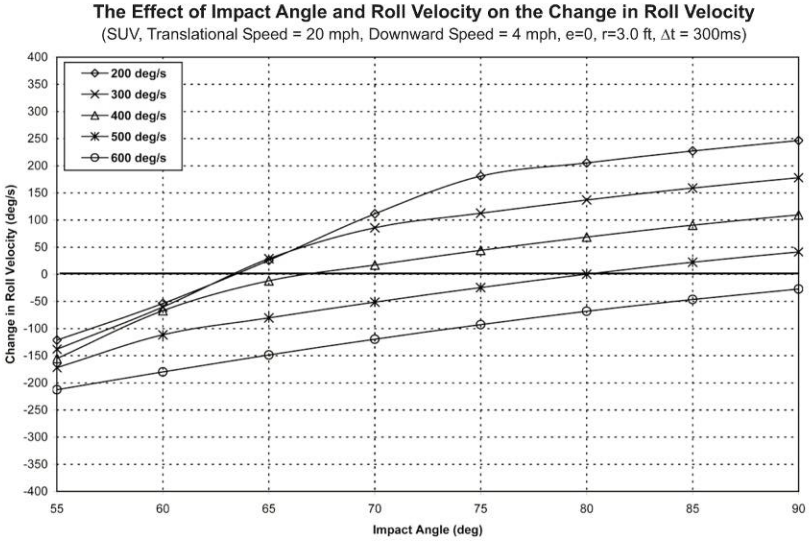
The Effect of Impact Angle and Roll Velocity on the Change in Roll Velocity
(SUV, Translational Speed = 20 mph, Downward Speed = 4 mph, e=0, r=3.0 ft, Δt = 300ms)
200 deg/s
300 deg/s
400 deg/s
500 deg/s
600 deg/s
Change in Roll Velocity (deg/s)
Impact Angle (deg)

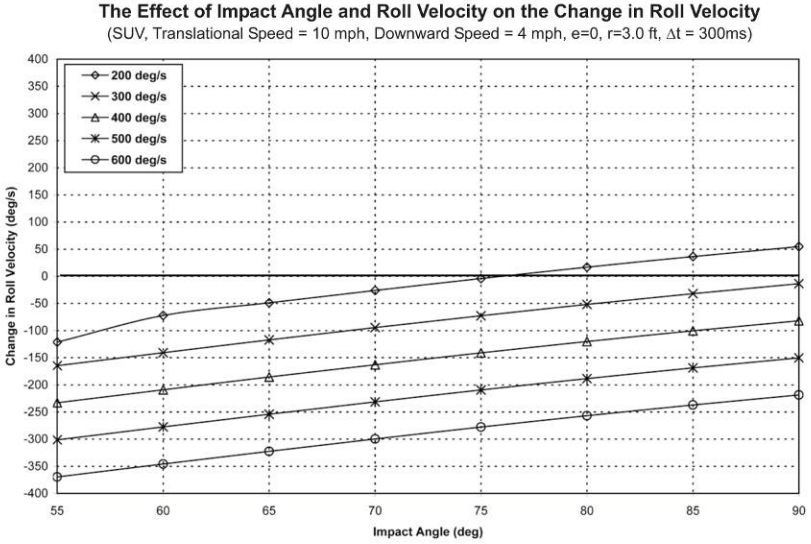
The Effect of Impact Angle and Roll Velocity on the Change in Roll Velocity
(SUV, Translational Speed = 10 mph, Downward Speed = 4 mph, e=0, r=3.0 ft, Δt = 300ms)
200 deg/s
300 deg/s
400 deg/s
500 deg/s
600 deg/s
Change in Roll Velocity (deg/s)
Impact Angle (deg)

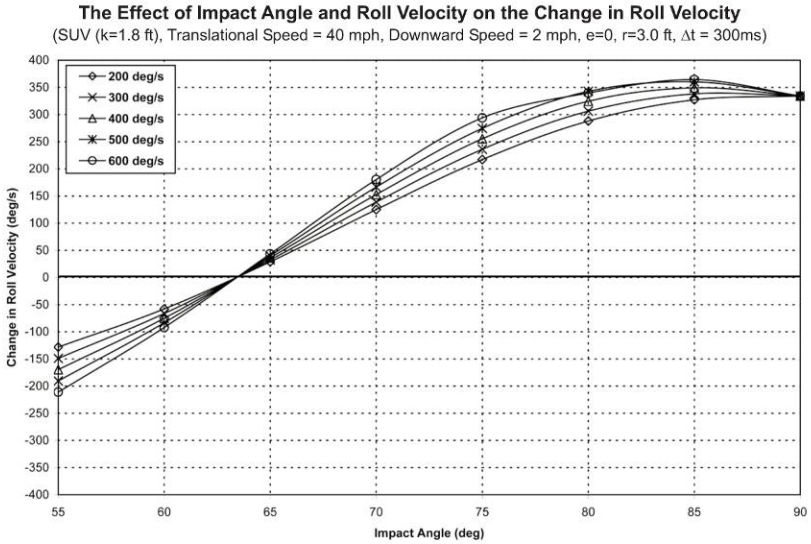
The Effect of Impact Angle and Roll Velocity on the Change in Roll Velocity
(SUV (k=1.8 ft), Translational Speed = 40 mph, Downward Speed = 2 mph, e=0, r=3.0 ft, Δt = 300ms)
200 deg/s
300 deg/s
400 deg/s
500 deg/s
600 deg/s
Change in Roll Velocity (deg/s)
Impact Angle (deg)

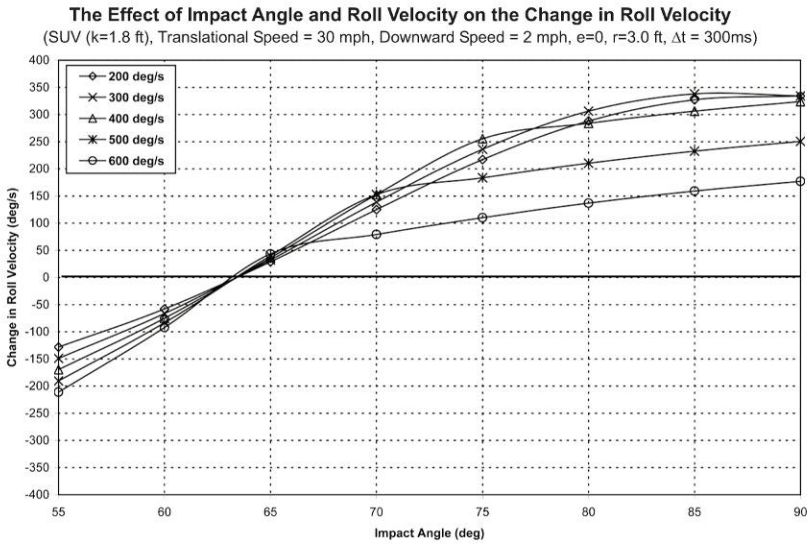
The Effect of Impact Angle and Roll Velocity on the Change in Roll Velocity
(SUV (k=1.8 ft), Translational Speed = 30 mph, Downward Speed = 2 mph, e=0, r=3.0 ft, Δt = 300ms)
200 deg/s
300 deg/s
400 deg/s
500 deg/s
600 deg/s
Change in Roll Velocity (deg/s)
Impact Angle (deg)

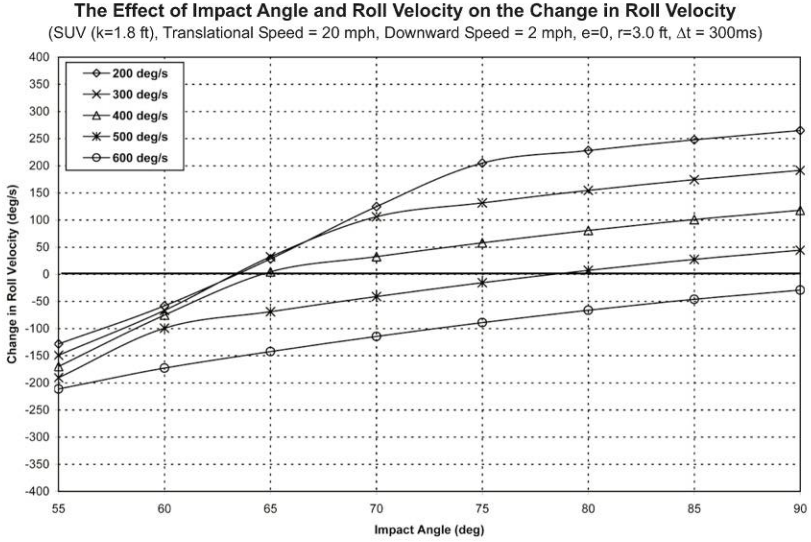
The Effect of Impact Angle and Roll Velocity on the Change in Roll Velocity
(SUV (k=1.8 ft), Translational Speed = 20 mph, Downward Speed = 2 mph, e=0, r=3.0 ft, Δt = 300ms)
200 deg/s
300 deg/s
400 deg/s
500 deg/s
600 deg/s
Change in Roll Velocity (deg/s)
Impact Angle (deg)

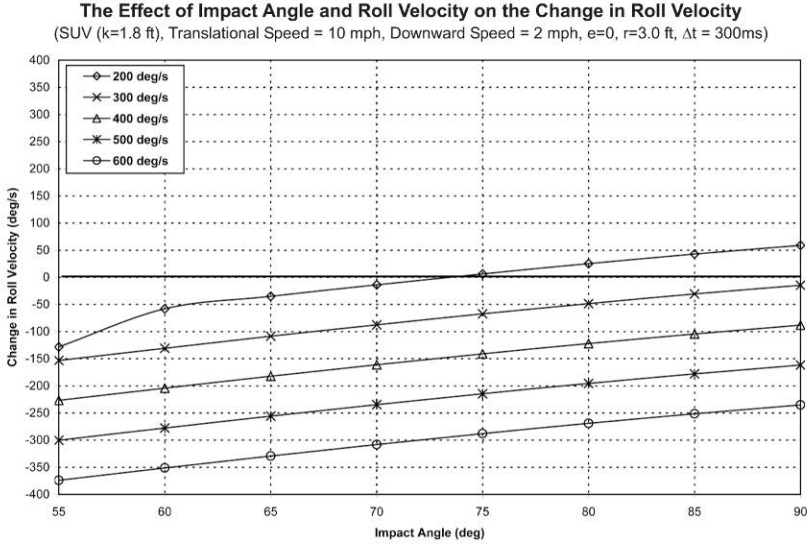
The Effect of Impact Angle and Roll Velocity on the Change in Roll Velocity
(SUV (k=1.8 ft), Translational Speed = 10 mph, Downward Speed = 2 mph, e=0, r=3.0 ft, Δt = 300ms)
200 deg/s
300 deg/s
400 deg/s
500 deg/s
600 deg/s
Change in Roll Velocity (deg/s)
Impact Angle (deg)

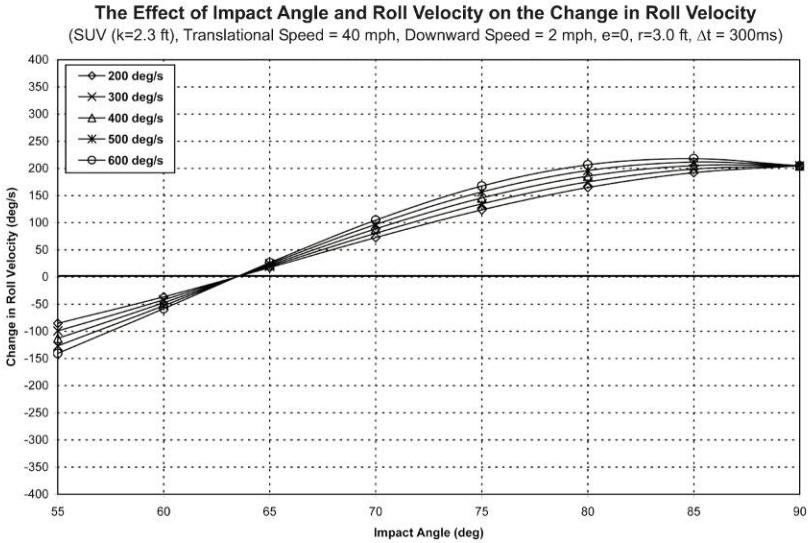
The Effect of Impact Angle and Roll Velocity on the Change in Roll Velocity
(SUV (k=2.3 ft), Translational Speed = 40 mph, Downward Speed = 2 mph, e=0, r=3.0 ft, Δt = 300ms)
200 deg/s
300 deg/s
400 deg/s
500 deg/s
600 deg/s
Change in Roll Velocity (deg/s)
Impact Angle (deg)

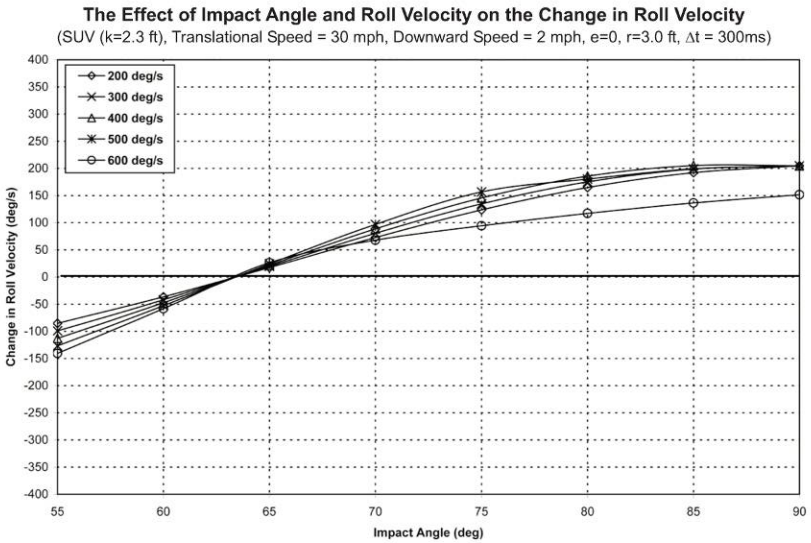
The Effect of Impact Angle and Roll Velocity on the Change in Roll Velocity
(SUV (k=2.3 ft), Translational Speed = 30 mph, Downward Speed = 2 mph, e=0, r=3.0 ft, Δt = 300ms)
200 deg/s
300 deg/s
400 deg/s
500 deg/s
600 deg/s
Change in Roll Velocity (deg/s)
Impact Angle (deg)

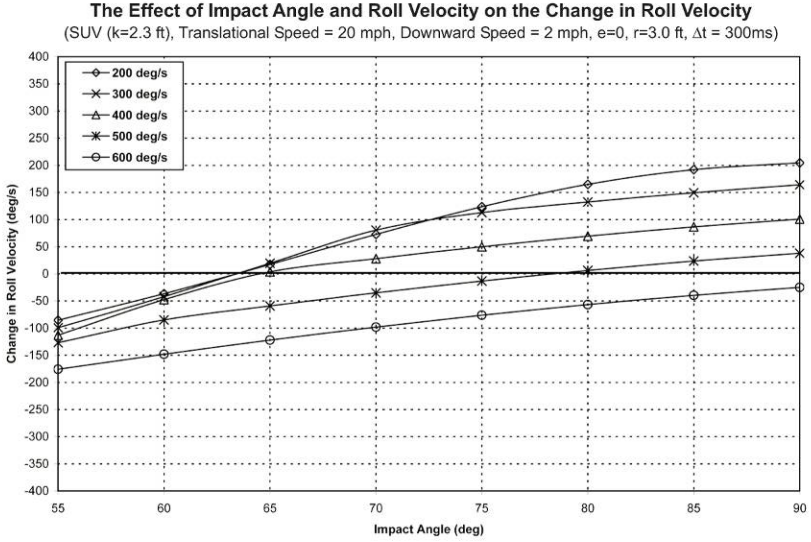
The Effect of Impact Angle and Roll Velocity on the Change in Roll Velocity
(SUV (k=2.3 ft), Translational Speed = 20 mph, Downward Speed = 2 mph, e=0, r=3.0 ft, Δt = 300ms)
200 deg/s
300 deg/s
400 deg/s
500 deg/s
600 deg/s
Change in Roll Velocity (deg/s)
Impact Angle (deg)

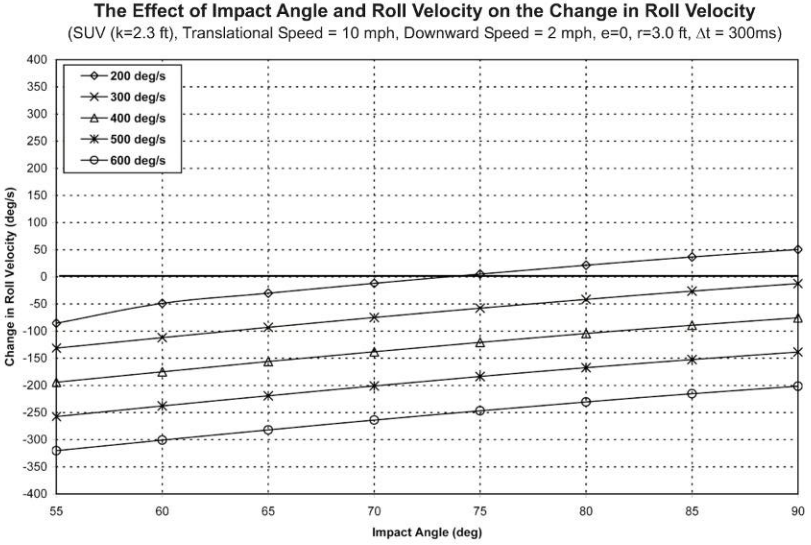
The Effect of Impact Angle and Roll Velocity on the Change in Roll Velocity
(SUV (k=2.3 ft), Translational Speed = 10 mph, Downward Speed = 2 mph, e=0, r=3.0 ft, Δt = 300ms)
200 deg/s
300 deg/s
400 deg/s
500 deg/s
600 deg/s
Change in Roll Velocity (deg/s)
Impact Angle (deg)

The Effect of Impact Angle and Roll Velocity on the Upward Velocity Change at the Contact
(SUV, Translational Speed = 40 mph, Downward Speed = 4 mph, e=0, r=3.0 ft, Δt = 300ms)

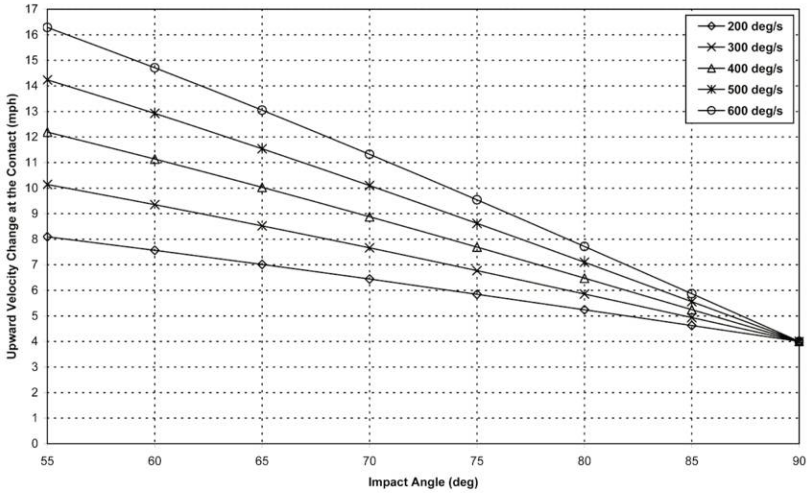

The Effect of Impact Angle and Roll Velocity on the Upward Velocity Change at the Contact
(SUV, Translational Speed = 30 mph, Downward Speed = 4 mph, e=0, r=3.0 ft, Δt = 300ms)

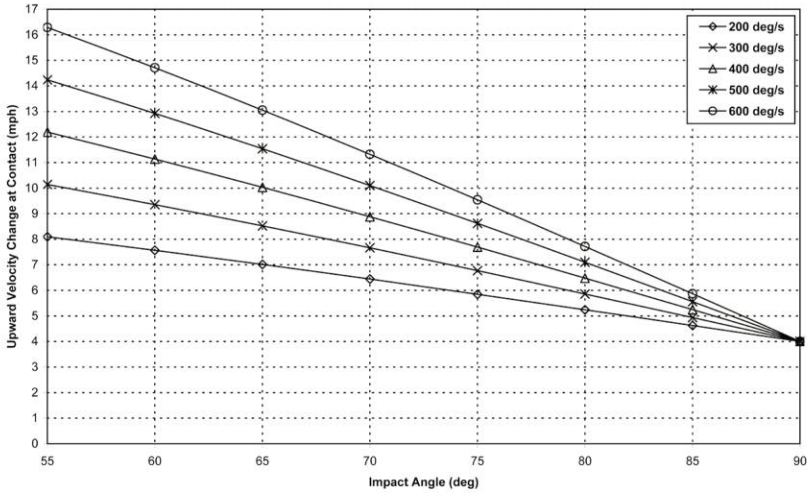

The Effect of Impact Angle and Roll Velocity on the Upward Velocity Change at Contact
(SUV, Translational Speed = 20 mph, Downward Speed = 4 mph, e=0, r=3.0 ft, Δt = 300ms)

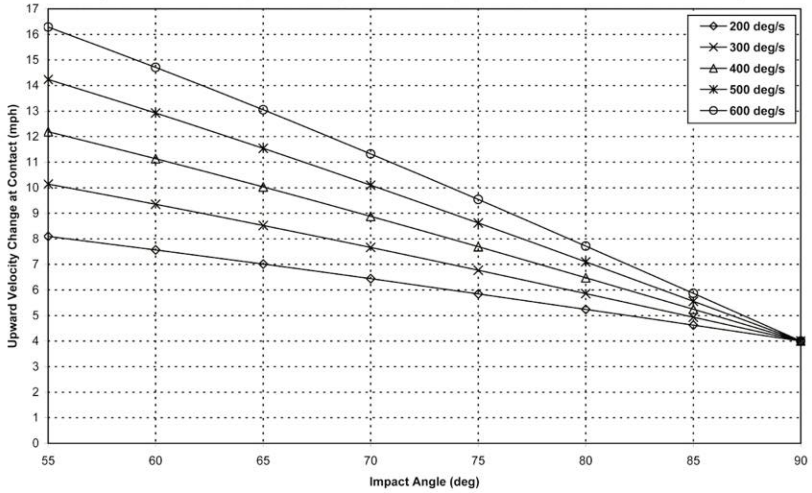

The Effect of Impact Angle and Roll Velocity on Upwared Velocity Change at Contact
(SUV, Translational Speed = 10 mph, Downward Speed = 4 mph, e=0, r=3.0 ft, Δt = 300ms)

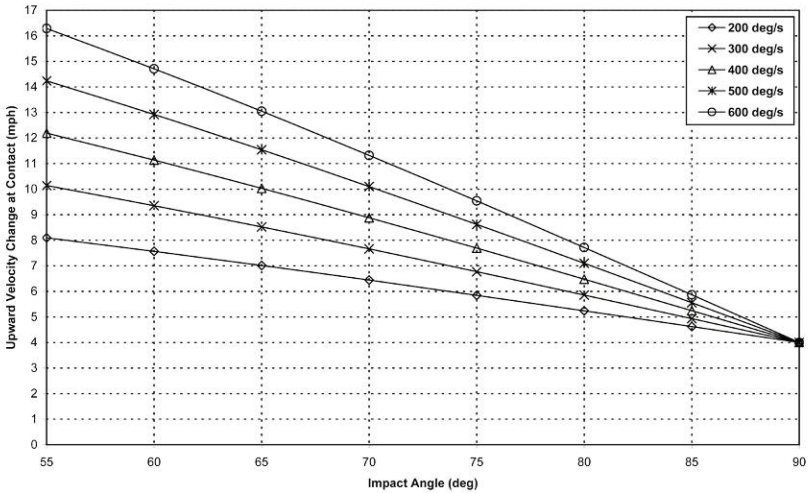

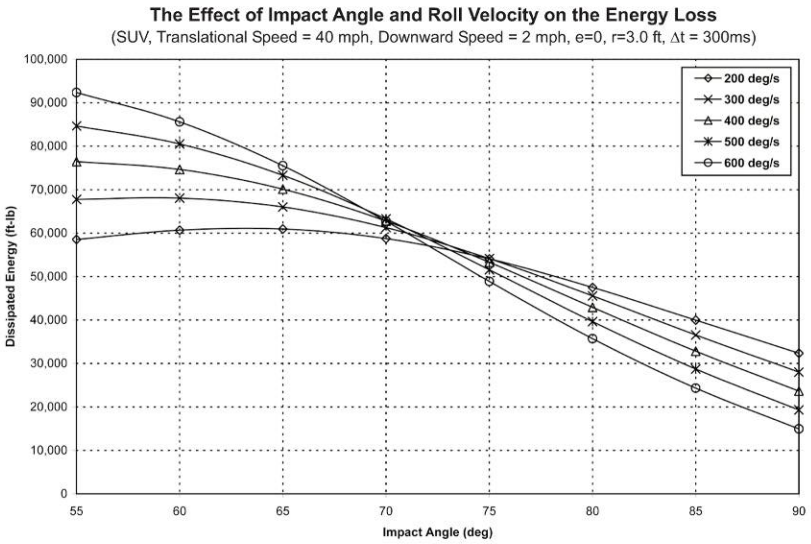

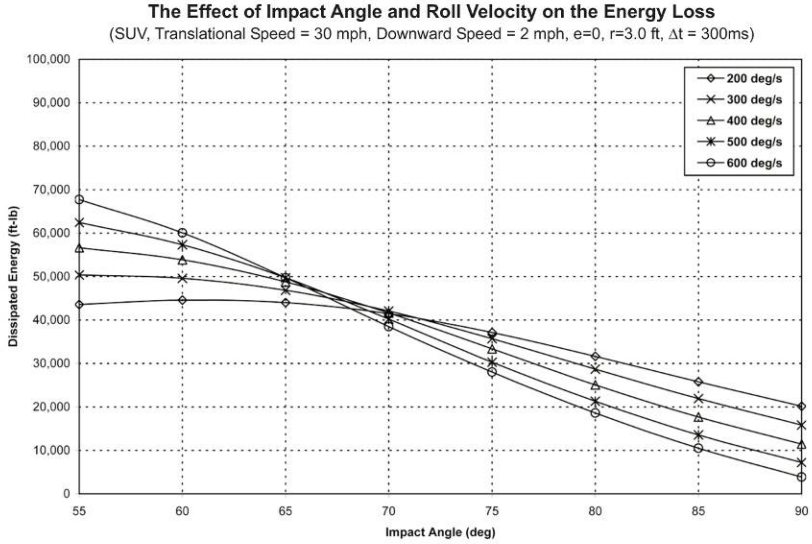

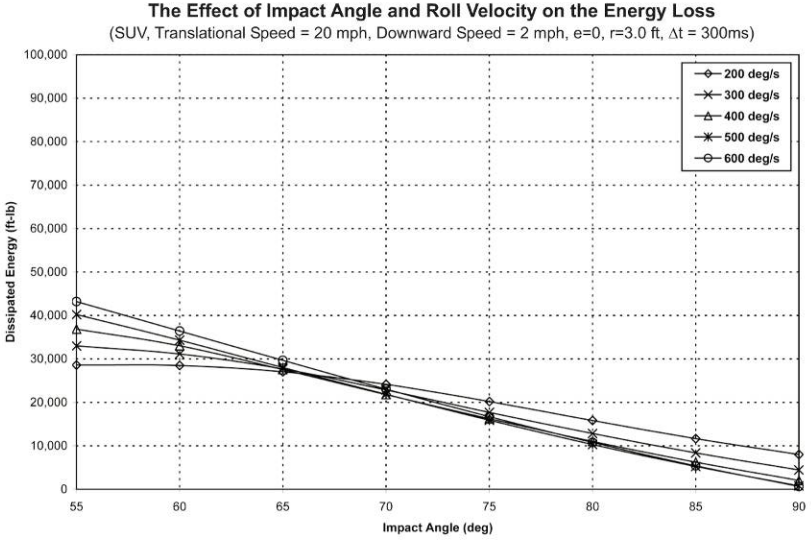

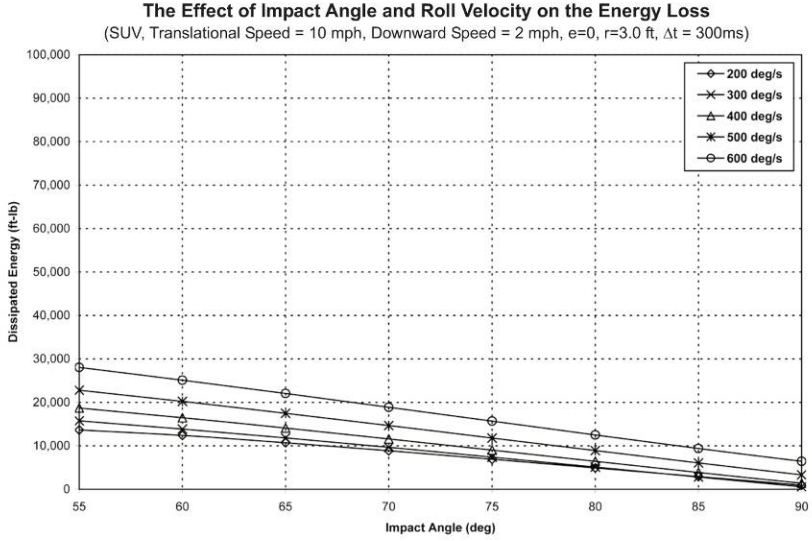

E1 - Vehicle-to-Ground Impact Scenarios (Energy Loss)